Bull Math Biol (2016) 78:138–168
DOI 10.1007/s11538-015-0133-1

Society for Mathematical Biology

ORIGINAL ARTICLE

Impact of Spring Bird Migration on the Range Expansion of *Ixodes scapularis* Tick Population

Xiaotian Wu[1] · **Gergely Röst**[2] · **Xingfu Zou**[3]

Received: 4 February 2015 / Accepted: 27 November 2015 / Published online: 18 December 2015

Abstract Many observational studies suggest that seasonal migratory birds play an important role in spreading *Ixodes scapularis*, a vector of Lyme disease, along their migratory flyways, and they are believed to be responsible for geographic range expansion of *I. scapularis* in Canada. However, the interplay between the dynamics of *I. scapularis* on land and migratory birds in the air is not well understood. In this study, we develop a periodic delay meta-population model which takes into consideration the local landscape for tick reproduction within patches and the times needed for ticks to be transported by birds between patches. Assuming that the tick population is endemic in the source region, we find that bird migration may boost an already established tick population at the subsequent region and thus increase the risk to humans, or bird migration may help ticks to establish in a region where the local landscape is not appropriate for ticks to survive in the absence of bird migration, imposing risks to public health. This theoretical study reveals that bird migration plays an important role in the geographic range expansion of *I. scapularis*, and therefore our findings may suggest some strategies for Lyme disease prevention and control.

✉ Xingfu Zou
xzou@uwo.ca

Xiaotian Wu
xtwu@shmtu.edu.cn

Gergely Röst
rost@math.u-szeged.hu

1 Department of Mathematics, Shanghai Maritime University, Shanghai 201306, China

2 Bolyai Institute, University of Szeged, Szeged H6720, Hungary

3 Department of Applied Mathematics, Western University, London, ON N6A 5B7, Canada

Keywords Bird migration · *Ixodes scapularis* · Range expansion · Meta-population model · Lyme disease

Mathematical Subject Classification 34C25 · 37N25 · 92D40

1 Introduction

Lyme disease is one of the most rapidly emerging tick-borne infectious zoonoses in temperate regions with the highest incidence occurring in Central-Eastern European countries, as well as in Northeastern and North-Central USA. Since 2003, more than 20,000 cases have been recorded annually in USA alone (Centers for Disease Control and Prevention 2014). In Canada, the number of cases is still very limited, but the absolute numbers of both the recognized Lyme-endemic regions and tick-established locations are increasing (Ogden et al. 2008, 2009). This is due to the sustained northward range expansion of the primary vector for the Lyme-pathogen—*Ixodes scapularis (I. scapularis)*, which is common in east of the Rocky Mountains in Canada (Anderson 1988; Ogden et al. 2008, 2009).

Habitat suitability, host abundance, climate change and tick dispersal are recognized as major factors in boosting the geographic range expansion of *I. scapularis* to the north (Ogden et al. 2008, 2009). Climate warming is believed to be a pivotal determinant due to the physiological/behavioral features of the *I. scapularis* life cycle (Ogden et al. 2006, 2008, 2014; Wu et al. 2013). Both the interstadial development (preoviposition period, preeclosion period, larva-to-nymph and nymph-to-adult) and questing activity (necessary for ticks to get the blood meal for developing to the next stage) are deeply influenced by the surrounding environment, especially temperature (Ogden et al. 2004, 2005). There have been some theoretical and empirical studies on the impact of climate change on the potential range expansion of the Lyme-vector (Brinkerhoff et al. 2011; Hasle et al. 2011; Madhav et al. 2004; Morshed et al. 2005; Ogden et al. 2006, 2014; Wu and Wu 2012). Moreover, it seems that the local terrestrial hosts of the vector are less likely to contribute to the long-distance range expansion due to their limited capacity of mobility and the short feeding periods. Some evidence seems to suggest that the migratory birds are, at least partially if not fully, responsible for the spread of Lyme-pathogen and Lyme-vector range expansion, due to their capacity for long-distance movement (Hasle et al. 2011; Morshed et al. 2005; Ogden et al. 2008; Rand et al. 1998).

In general, ground-feeding birds such as song sparrows and American robins are common hosts for hematophagous organisms (Comstedt et al. 2006). At least 71 bird species in North America are parasitized by immature (larval and nymphal) Lyme-vector, and 14 % of the studied birds were infested by at least one larva or nymph (Brinkerhoff et al. 2011). It is estimated that around 50–175 millions of immature *I. scapularis* are dispersing through or across Canada transported by migratory birds during their spring migration (Ogden et al. 2008). The seasonal migrations of these ground-feeding birds are known to be synchronized with the seeking periods of immature *I. scapularis* (Bird Life international 2013). Moreover, it is observed that the most established *I. scapularis* populations in Canada are not geographically continuously

distributed, but are actually isolated from each other and are mainly adjacent to the US border, mostly located along the shores of the Great Lakes in Ontario, Lake of Woods in Manitoba, and the coast of Nova Scotia (Ogden et al. 2008). However, the interplay between *I. scapularis* on land and the migratory birds in the air is not well understood yet. Better understanding of the mechanisms and processes of range expansion of *I. scapularis* transported by migratory birds is thus of both theoretical and practical significance for designing public health policies on surveillance, prevention and control.

In this study, we develop a mathematical model, which is a patch-based periodic system of delay differential equations with multiple delays accounting for the times needed for larvae or nymphs to be transported by migratory birds between consecutive locations during spring migration. By analyzing this model, we examine the effects of the heterogeneous environment and the migration ability of birds to connect source regions with subsequent regions (stopovers) for different life stages of ticks with various patterns of seasonal abundance. The model is mathematically tractable by the theory of periodic delay differential equations and monotone dynamical systems.

The rest of the paper is organized as follows. In the next section, we present the multi-patch model in a general setting of $N > 1$ patches. Section 3 concerns with the fundamental properties of our model such as boundedness and nonnegativity of solutions. In Sect. 4, the basic reproduction ratio of the tick population at the source region is identified and shown to be a threshold parameter with respect to the local population dynamics. Then the tick population dynamics is analyzed in the subsequent locations. In Sect. 5, we perform numerical simulations to investigate the ability of bird migration on increasing the risk of Lyme disease to humans for two successive patches. The paper ends with a brief discussion of our findings and their implications.

2 General Meta-population Model in N Patches

Migratory birds can have complicated flyways; however, the transportation of ticks carried by birds can be considered on a unidirectional route. This is because the seeking period of immature *I. scapularis* overlaps with the bird spring migration season when birds fly from south to north, while they are inactive in late fall when birds migrate from north to south. In particular, Brinkerhoff et al. (2011) reported that the most likely time to encounter larval *I. scapularis* is between late May and early July when bird species migrate from south to north. Thus, we only model the spatial dispersal of *I. scapularis* population transported by migratory birds during spring migration from south to north, in one direction. To capture the heterogeneity of the landscape along such a migration route, we consider some consecutive locations which are stopovers for the birds. We construct a deterministic meta-population model over N patches, as the birds pass along their migration routes. Within a single patch, it is a system of delay differential equations consisting of 14 equations, with seasonally varying parameters representing the local environment. Each equation corresponds to the tick population at a specific stage of development of the tick's life cycle.

Ixodes scapularis has three main stages after the egg stage, and these are larva, nymph and adult, and it has a relatively long life span of around 2 years. Each stage

further breaks down to three states: questing, feeding and engorged. In order to complete their life cycle, ticks in each stage have to manage to attach to a host and get the necessary blood meal. Since *I. scapularis* is a three-host generalist tick, based on the same consideration as in Wu et al. (2013), we assume that both rodents and migratory birds serve as the hosts for immature ticks, while the adult ticks feed only on deer (mainly white-tailed deer). For simplicity, we assume that the populations of the rodents and deer in patch i ($i = 1, \ldots, N$) remain constants, denoted by R_i and D_i, respectively. Let $B_i(t)$ be the population of birds in patch i at time t, which varies periodically with a 1 year period.

Following the framework of Wu et al. (2013), we divide the vector life cycle into 14 states as follows: egg-laying females (ELAF), eggs (E), hardening larvae (HL), questing larvae (QL), feeding larvae on rodents (FLr), feeding larvae on birds (FLb), engorged larvae (EL), questing nymphs (QN), feeding nymphs on rodents (FNr), feeding nymphs on birds (FNb), engorged nymphs (EN), questing adults (QA), feeding adult females on deer (FAF) and engorged adult females (EAF) (see Fig. 1; Table 1). The equations for the rate of change of tick population in each state reflect that they may migrate either into or out of the patch, produce offspring, develop to next state or die. In terms of the above stages and states, we need fourteen variables to denote the respective subpopulations, and these variables are listed and explained in Table 1.

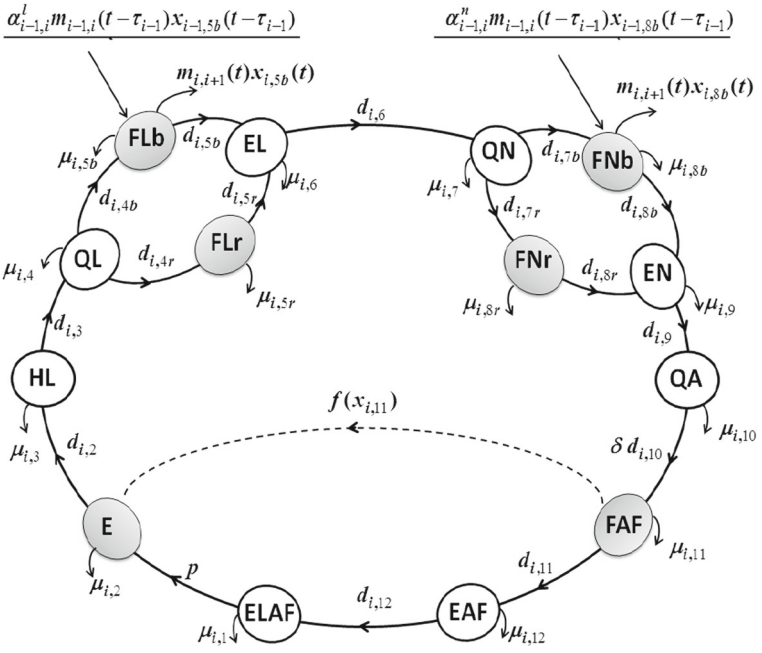

Fig. 1 Flowchart of *I. scapularis* tick population at patch i ($1 \le i \le N$) with dispersion from (to) patch $i-1$ (patch $i+1$) transported by spring migratory birds. We assume that there is no tick immigration at patch 1 and no tick emigration at patch N due to spring bird migration, which means that $m_{0,1} = m_{N,N+1} = 0$ in the system

Table 1 Definition and description of each variable in the model (1) at patch i

Variable	Description of each variable	Notation
$x_{i,1}(t)$	Number of egg-laying females at time t	ELAF
$x_{i,2}(t)$	Number of eggs at time t	E
$x_{i,3}(t)$	Number of hardening larvae at time t	HL
$x_{i,4}(t)$	Number of questing larvae at time t	QL
$x_{i,5r}(t)$	Number of feeding larvae on rodents at time t	FLr
$x_{i,5b}(t)$	Number of feeding larvae on birds at time t	FLb
$x_{i,6}(t)$	Number of engorged larvae at time t	EL
$x_{i,7}(t)$	Number of questing nymphs at time t	QN
$x_{i,8r}(t)$	Number of feeding nymphs on rodents at time t	FNr
$x_{i,8b}(t)$	Number of feeding nymphs on birds at time t	FNb
$x_{i,9}(t)$	Number of engorged nymphs at time t	EN
$x_{i,10}(t)$	Number of questing adults at time t	QA
$x_{i,11}(t)$	Number of feeding adult females at time t	FAF
$x_{i,12}(t)$	Number of engorged adult females at time t	EAF

Then, the population dynamics of the ticks at patch i is governed by

$$
\begin{aligned}
x'_{i,1}(t) &= d_{i,12}(t)x_{i,12}(t) - \mu_{i,1}(t)x_{i,1}(t),\\
x'_{i,2}(t) &= p(t)f(x_{i,11}(t))x_{i,1}(t) - d_{i,2}(t)x_{i,2}(t) - \mu_{i,2}(t)x_{i,2}(t),\\
x'_{i,3}(t) &= d_{i,2}(t)x_{i,2}(t) - d_{i,3}(t)x_{i,3}(t) - \mu_{i,3}(t)x_{i,3}(t),\\
x'_{i,4}(t) &= d_{i,3}(t)x_{i,3}(t) - d_{i,4r}(t, R_i)x_{i,4}(t) - d_{i,4b}(t, B_i(t))x_{i,4}(t) - \mu_{i,4}(t)x_{i,4}(t),\\
x'_{i,5r}(t) &= d_{i,4r}(t, R_i)x_{i,4}(t) - d_{i,5r}(t)x_{i,5r}(t) - \mu_{i,5r}(t, x_{i,5r}(t))x_{i,5r}(t),\\
x'_{i,5b}(t) &= d_{i,4b}(t, B_i(t))x_{i,4}(t) + \boxed{\alpha^l_{i-1,i}(t)m_{i-1,i}(t-\tau_{i-1})x_{i-1,5b}(t-\tau_{i-1})}\\
&\quad - \boxed{m_{i,i+1}(t)x_{i,5b}(t)} - d_{i,5b}(t)x_{i,5b}(t) - \mu_{i,5b}(t, x_{i,5b}(t))x_{i,5b}(t),\\
x'_{i,6}(t) &= d_{i,5r}(t)x_{i,5r}(t) + d_{i,5b}(t)x_{i,5b}(t) - d_{i,6}(t)x_{i,6}(t) - \mu_{i,6}(t)x_{i,6}(t),\\
x'_{i,7}(t) &= d_{i,6}(t)x_{i,6}(t) - d_{i,7r}(t, R_i)x_{i,7}(t) - d_{i,7b}(t, B_i(t))x_{i,7}(t) - \mu_{i,7}(t)x_{i,7}(t),\\
x'_{i,8r}(t) &= d_{i,7r}(t, R_i)x_{i,7}(t) - d_{i,8r}(t)x_{i,8r}(t) - \mu_{i,8r}(t, x_{i,8r}(t))x_{i,8r}(t),\\
x'_{i,8b}(t) &= d_{i,7b}(t, B_i(t))x_{i,7}(t) + \boxed{\alpha^n_{i-1,i}(t)m_{i-1,i}(t-\tau_{i-1})x_{i-1,8b}(t-\tau_{i-1})}\\
&\quad - \boxed{m_{i,i+1}(t)x_{i,8b}(t)} - d_{i,8b}(t)x_{i,8b}(t) - \mu_{i,8b}(t, x_{i,8b}(t))x_{i,8b}(t),\\
x'_{i,9}(t) &= d_{i,8r}(t)x_{i,8r}(t) + d_{i,8b}(t)x_{i,8b}(t) - d_{i,9}(t)x_{i,9}(t) - \mu_{i,9}(t)x_{i,9}(t),\\
x'_{i,10}(t) &= d_{i,9}(t)x_{i,9}(t) - d_{i,10}(t, D_i)x_{i,10}(t) - \mu_{i,10}(t)x_{i,10}(t),\\
x'_{i,11}(t) &= \delta d_{i,10}(t, D_i)x_{i,10}(t) - d_{i,11}(t)x_{i,11}(t) - \mu_{i,11}(t, x_{i,11}(t))x_{i,11}(t),\\
x'_{i,12}(t) &= d_{i,11}(t)x_{i,11}(t) - d_{i,12}(t)x_{i,12}(t) - \mu_{i,12}(t)x_{i,12}(t),
\end{aligned}
\tag{1}
$$

where

$$\alpha^l_{i-1,i}(t) = \exp\left(-\int_{t-\tau_{i-1}}^{t} (\mu^l_{i-1,i}(\eta) + \mu^b_{i-1,i}(\eta) + d^l_{i-1,i}(\eta))\,\mathrm{d}\eta\right),$$
$$\alpha^n_{i-1,i}(t) = \exp\left(-\int_{t-\tau_{i-1}}^{t} (\mu^n_{i-1,i}(\eta) + \mu^b_{i-1,i}(\eta) + d^n_{i-1,i}(\eta))\,\mathrm{d}\eta\right),$$

represent the survival probabilities of feeding larvae and nymphs being attached to birds flying from patch $i-1$ toward patch i, from time $t-\tau_{i-1}$ to time t, respectively. The terms $\alpha^l_{i-1,i}(t)m_{i-1,i}(t-\tau_{i-1})x_{i-1,5b}(t-\tau_{i-1})$ and $\alpha^n_{i-1,i}(t)m_{i-1,i}(t-\tau_{i-1})x_{i-1,8b}(t-\tau_{i-1})$ account for the influxes of feeding larvae and nymphs at time t entering patch i after being transported by the birds from previous patch $i-1$. We assume that ticks are capable of being developed during flight; however, once ticks are full engorged, they fall off and disappear from our system (Ogden et al. 2008). For the reader's convenience, the biological interpretation of all parameters is given in Table 2 and Table 3, and the detailed derivation of the model (1) is presented in "Appendix 1." Given their biological meanings, we assume in the rest of the paper that $f(\cdot)$ is a decreasing function, while $\mu_{i,5r}(t,\cdot)$, $\mu_{i,5b}(t,\cdot)$, $\mu_{i,8r}(t,\cdot)$, $\mu_{i,8b}(t,\cdot)$ and $\mu_{i,11}(t,\cdot)$ are continuous and increasing functions with respect to their respective state variables.

It is natural to assume that all parameters are nonnegative and periodic with period $\omega = 365$ days, and some of them can possibly be positive only in some subinterval within a period, due to seasonal on-and-off effects. In the rest of the paper, we analyze the model represented by system (1).

3 Nonnegativity and Boundedness of Solutions

We start by addressing the nonnegativity and boundedness of the solutions under suitable initial conditions. For simplicity of notations, we introduce the following three sets: $\mathcal{A} = \{1,\ldots,N\}$, $\mathcal{B} = \{2,3,5r,5b,6,8r,8b,9,10,11,12\}$ and $\mathcal{C} = \{1,2,3,4,5r,5b,6,7,8r,8b,9,10,11,12\}$

Proposition 3.1 *Assuming Lipschitz continuity of each nonlinear term, for any given set of nonnegative initial functions for the fourteen variables, the system* (1) *has a unique solution which exists globally and is nonnegative and bounded for all* $t \geq 0$.

Proof The existence and uniqueness of a solution follow directly from the fundamental theory of delay differential equations (see, e.g., Hale and Verduyn Lunel 1993). The nonnegativity of each $x_{i,j}(t)$ for $i \in \mathcal{A}$ and $j \in \mathcal{C}$ follows immediately from Theorem 5.2.1 on page 81 of Smith (1995). It remains to prove the boundedness which will also imply that the existence of the solution is global.

Firstly, at a stage j that is neither feeding larvae nor feeding nymphs (i.e., $j \in \mathcal{C} \setminus \{5r,5b,8r,8b\}$), the total number of ticks across all patches at this stage at time t is given by

$$V_j(t) = \sum_{i=1}^{N} x_{i,j}(t), \quad j \in \mathcal{C} \setminus \{5r,5b,8r,8b\}. \tag{2}$$

Table 2 Definition and description of model parameters relevant to development and migration of the Lyme-ticks (the unit of each rate is per day)

Model parameter	Description of each parameter (value, reference)
$d_{i,2}(t)$	Development rate from eggs to hardening larvae (estimate, Wu et al. 2013)
$d_{i,3}(t)$	Development rate from hardening larvae to questing (1/21, Ogden et al. 2005)
$d_{i,4r}(t, R_i)$	Host attaching rate for questing larvae to rodents (estimate, Wu et al. 2013)
$d_{i,4b}(t, B_i(t))$	Host attaching rate for questing larvae to birds (estimate, Wu et al. 2013)
$d_{i,5r}(t)$	Development rate for feeding larvae on rodents (1/3, Ogden et al. 2005)
$d_{i,5b}(t)$	Development rate for feeding larvae on birds (1/3, Ogden et al. 2005)
$d_{i,6}(t)$	Development rate for engorged larvae (estimate, Wu et al. 2013)
$d_{i,7r}(t, R_i)$	Host attaching rate for questing nymphs on rodents (estimate, Wu et al. 2013)
$d_{i,7b}(t, B_i(t))$	Host attaching rate for questing nymphs on birds (estimate, Wu et al. 2013)
$d_{i,8r}(t)$	Development rate for feeding nymphs on rodents (1/5, Ogden et al. 2005)
$d_{i,8b}(t)$	Development rate for feeding nymphs on birds (1/5, Ogden et al. 2005)
$d_{i,9}(t)$	Development rate for engorged nymphs (estimate, Wu et al. 2013)
$d_{i,10}(t, D_i)$	Host attaching rate for questing adults (estimate, Wu et al. 2013)
$d_{i,11}(t)$	Development rate for feeding adult females (1/10, Ogden et al. 2005)
$d_{i,12}(t)$	Development rate for engorged females (estimate, Wu et al. 2013)
R_i	Number of rodents (200, Ogden et al. 2005)
D_i	Number of deer (20, Ogden et al. 2005)
$B_i(t)$	Number of birds at patch i at time t (varied)
$d^l_{i-1,i}(t)$	Development rate of larvae on birds in the flight from patch $i-1$ to i (1/3, Ogden et al. 2005)
$d^n_{i-1,i}(t)$	Development rate of nymphs on birds in the flight from patch $i-1$ to i (1/5, Ogden et al. 2005)
τ_{i-1}	Flight time of birds from patch $i-1$ to patch i
$m_{i-1,i}(t)$	Migration rate of birds at time t from patch $i-1$ to patch i
$\mu^b_{i-1,i}(t)$	Mortality of birds in flight from patch $i-1$ to i
$\mu^l_{i-1,i}(t)$	Mortality of feeding larvae on birds in the flight from patch $i-1$ to patch i
$\mu^n_{i-1,i}(t)$	Mortality of feeding nymphs on birds in the flight from patch $i-1$ to patch i

Table 3 Definition and description of parameters relevant to birth and death of the Lyme-ticks (the unit of each rate is per day)

Model parameter	Description of each model parameter (value, reference)
$p(t)$	Number of eggs produced by egg-laying adult females (3000, Ogden et al. 2005)
$f(x_{i,11}(t))$	Fecundity reduction factor $(1-[0.01+0.04\ln(1.01+\frac{x_{i,11}(t)}{D_i})]$, Ogden et al. 2005)
δ	Sex ratio of *I. scapularis* (0.5, Ogden et al. 2005)
$\mu_{i,1}(t)$	Mortality rate of egg-laying adult females (1, Wu et al. 2013)
$\mu_{i,2}(t)$	Mortality rate of eggs (0.002, Ogden et al. 2005)
$\mu_{i,3}(t)$	Mortality rate of hardening larvae (0.006, Ogden et al. 2005)
$\mu_{i,4}(t)$	Mortality rate of questing larvae (0.006, Ogden et al. 2005)
$\mu_{i,6}(t)$	Mortality rate of engorged larvae (0.006, Ogden et al. 2005)
$\mu_{i,7}(t)$	Mortality rate of questing nymphs (0.006, Ogden et al. 2005)
$\mu_{i,9}(t)$	Mortality rate of engorged nymphs (0.002, Ogden et al. 2005)
$\mu_{i,10}(t)$	Mortality rate of questing adults (0.006, Ogden et al. 2005)
$\mu_{i,12}(t)$	Mortality rate of engorged adult females (0.0001, Ogden et al. 2005)
$\mu_{i,5r}(t, x_{i,5r}(t))$	Mortality rate of feeding larvae on rodents $(0.65+0.049\ln\frac{1.01+x_{i,5r}}{R_i}$, Ogden et al. 2005)
$\mu_{i,5b}(t, x_{i,5b}(t))$	Mortality rate of feeding larvae on birds $(0.65+0.049\ln\frac{1.01+x_{i,5b}}{B_i(t)}$, Ogden et al. 2005)
$\mu_{i,8r}(t, x_{i,8r}(t))$	Mortality rate of feeding nymphs on rodents $(0.55+0.049\ln\frac{1.01+x_{i,8r}}{R_i}$, Ogden et al. 2005)
$\mu_{i,8b}(t, x_{i,8b}(t))$	Mortality rate of feeding nymphs on birds $(0.55+0.049\ln\frac{1.01+x_{i,8b}}{B_i(t)}$, Ogden et al. 2005)
$\mu_{i,11}(t, x_{i,11}(t))$	Mortality rate of feeding adults on deer $(0.5+0.049\ln\frac{1.01+x_{i,11}(t)}{D_i}$, Ogden et al. 2005)

Tracking the total numbers of ticks at the feeding larvae and feeding nymphs states are more complicated due to transportation between patches by birds. We only present the details for the feeding nymphs, and the tracking of population of feeding larvae can be similarly obtained.

Following the "Appendix 1," we let $\rho_{i,i+1}(t, a, y)$ be the density (w.r.t. feeding age a) of feeding nymphs on birds flying from patch i to patch $i+1$ that is at a location with distance y from patch i at time t, $y \in [0, l_{i,i+1}]$ where $l_{i,i+1}$ is the distance from patch i to patch $i+1$. Then the total number of feeding nymphs on birds at time t at location y between patch i and patch $i+1$ is given by

$$W_{i,i+1}(t, y) := \int_0^\infty \rho_{i,i+1}(t, a, y)\, \mathrm{d}a.$$

It follows from Eq. (25) in "Appendix 1" that

$$\begin{aligned}\frac{\partial W_{i,i+1}(t,y)}{\partial t} &= -v_{i,i+1}\frac{\partial W_{i,i+1}(t,y)}{\partial y} - \mu^b_{i,i+1}(t)W_{i,i+1}(t,y)\\ &\quad - \mu^n_{i,i+1}(t)W_{i,i+1}(t,y) - d^n_{i,i+1}(t)W_{i,i+1}(t,y).\end{aligned} \tag{3}$$

Here, we have used the biologically meaningful facts that $\rho_{i,i+1}(t,0,y) = \rho_{i,i+1}(t,\infty,y) = 0$. Then the total number of feeding nymphs feeding on birds at time t, on both ground (patches) and flight (flying birds) is given by

$$x_{\text{tot},8b}(t) = \sum_{i=1}^{N} x_{i,8b}(t) + \sum_{i=1}^{N-1}\int_0^{l_{i,i+1}} W_{i,i+1}(t,y)\,\mathrm{d}y. \tag{4}$$

For the sake of simplicity, $\overline{h}_j$ and $\underline{h}_j$ are defined by

$$\overline{h}_j = \max_{i\in\mathcal{A}}\left\{\max_{t\in[0,\omega]} h_{i,j}(t)\right\}, \qquad \underline{h}_j = \min_{i\in\mathcal{A}}\left\{\min_{t\in[0,\omega]} h_{i,j}(t)\right\} \tag{5}$$

for a periodic function $h_{i,j}(t)$ of period ω. Straightforward calculation of (4) leads to

$$\begin{aligned}x'_{\text{tot},8b}(t) &= \sum_{i=1}^{N} d_{i,7b}(t, B_i(t))x_{i,7}(t) - \sum_{i=1}^{N} d_{i,8b}(t)x_{i,8b}(t)\\ &\quad - \sum_{i=1}^{N}\mu_{i,8b}(t,x_{i,8b}(t))x_{i,8b}(t)\\ &\quad - \sum_{i=1}^{N-1}\left(\mu^b_{i,i+1}(t) + \mu^n_{i,i+1}(t) + d^n_{i,i+1}(t)\right)\int_0^{l_{i,i+1}} W_{i,i+1}(t,y)\,\mathrm{d}y\\ &\le \overline{d}_{7b}\sum_{i=1}^{N} x_{i,7}(t) - \underline{d}_{8b}\sum_{i=1}^{N} x_{i,8b}(t) - \underline{\mu}_{8b}\sum_{i=1}^{N} x_{i,8b}(t)\\ &\quad -\hat{\mu}\sum_{i=1}^{N-1}\int_0^{l_{i,i+1}} W_{i,i+1}(t,y)\,\mathrm{d}y\\ &\le \overline{d}_{7b}V_7(t) - \underline{\mu}x_{\text{tot},8b}(t),\end{aligned} \tag{6}$$

where

$$\begin{aligned}\underline{\mu}_{8b} &= \min_{i\in\mathcal{A}}\left\{\min_{t\in[0,\omega]}\mu_{i,8b}(t,0)\right\}, \quad \underline{\mu} = \min\{\underline{d}_{8b} + \underline{\mu}_{8b}, \hat{\mu}\},\\ \hat{\mu} &= \min_{i\in\{1,\ldots,N-1\}}\left\{\min_{t\in[0,\omega]}(\mu^b_{i,i+1}(t) + \mu^n_{i,i+1}(t) + d^n_{i,i+1}(t))\right\}.\end{aligned}$$

Therefore, the total number of feeding nymphs (on birds or rodents, on ground or in flight), denoted by $V_8(t) = x_{\text{tot},8b}(t) + \sum_{i=1}^{N} x_{i,8r}(t)$, satisfies

$$\begin{aligned} V_8'(t) &= x_{\text{tot},8b}'(t) + \sum_{i=1}^{N} x_{i,8r}'(t) = x_{\text{tot},8b}'(t) \\ &\quad + \sum_{i=1}^{N} \left[d_{i,7r}(t, R_i) x_{i,7}(t) - d_{i,8r}(t) x_{i,8r}(t) - \mu_{i,8r}(t, x_{i,8r}(t)) x_{i,8r}(t) \right] \\ &\le (\overline{d}_{7r} + \overline{d}_{7b}) V_7(t) - (\underline{d}_{8r} + \underline{\mu}_{8r}) \sum_{i=1}^{N} x_{i,8r}(t) - \underline{\mu} x_{\text{tot},8b}(t) \\ &\le (\overline{d}_{7r} + \overline{d}_{7b}) V_7(t) - \mu_8 V_8(t), \end{aligned} \tag{7}$$

where $\underline{\mu}_{8r} = \min_{i \in \mathcal{A}} \left\{ \min_{t \in [0,\omega]} \mu_{i,8r}(t, 0) \right\}$ and $\mu_8 = \min\{\underline{d}_{8r} + \underline{\mu}_{8r}, \underline{\mu}\}$.

Similarly, there exists a positive number μ_5 such that the total number of feeding larvae, denoted by $V_5(t)$, satisfies

$$V_5'(t) \le (\overline{d}_{4r} + \overline{d}_{4b}) V_4(t) - \mu_5 V_5(t). \tag{8}$$

Next we consider the change rate of the total number of feeding adult females in all patches, denoted by V_{11}. Denoting

$$\Delta_{11} = \min_{i \in \mathcal{A}} \left\{ \min_{t \in [0,\omega]} \frac{\partial \mu_{i,11}(t, 0)}{\partial x_{i,11}} \right\},$$

we have the following estimate

$$\begin{aligned} V_{11}'(t) &= \sum_{i=1}^{N} x_{i,11}'(t) \\ &= \sum_{i=1}^{N} \left[\delta d_{i,10}(t, D_i) x_{i,10}(t) - d_{i,11}(t) x_{i,11}(t) - \mu_{i,11}(t, x_{i,11}(t)) x_{i,11}(t) \right] \\ &\le \delta \overline{d}_{10} V_{10}(t) - \underline{d}_{11} V_{11}(t) - \sum_{i=1}^{N} \mu_{i,11}(t, x_{i,11}(t)) x_{i,11}(t) \\ &\le \delta \overline{d}_{10} V_{10}(t) - \underline{d}_{11} V_{11}(t) - \sum_{i=1}^{N} \frac{\partial \mu_{i,11}(t, 0)}{\partial x_{i,11}} x_{i,11}^2(t) \\ &\le \delta \overline{d}_{10} V_{10}(t) - \underline{d}_{11} V_{11}(t) - \Delta_{11} \sum_{i=1}^{N} x_{i,11}^2(t) \\ &\le \delta \overline{d}_{10} V_{10}(t) - \underline{d}_{11} V_{11}(t) - \frac{\Delta_{11}}{N} \left(\sum_{i=1}^{N} x_{i,11}(t) \right)^2 \end{aligned}$$

$$= \delta\overline{d}_{10}V_{10}(t) - \underline{d}_{11}V_{11}(t) - \frac{\Delta_{11}}{N}V_{11}^2(t) \tag{9}$$

by the property of $\mu_{i,11}(t, x_{i,11}(t))$ and the Cauchy–Schwarz inequality.

By similar argument, we can also establish the estimates for the total numbers of ticks in other remaining stages:

$$\begin{aligned} V_1'(t) &\le \overline{d}_{12}V_{12}(t) - \underline{\mu}_1 V_1(t), \\ V_2'(t) &\le \overline{p}f(0)V_1(t) - (\underline{d}_2 + \underline{\mu}_2)V_2(t), \\ V_i'(t) &\le \overline{d}_{i-1}V_{i-1}(t) - (\underline{d}_i + \underline{\mu}_i)V_i(t), \ \ i = 3, 4, 6, 7, 9, 10, 12. \end{aligned} \tag{10}$$

Note that the constant coefficients are obtained in the way (5) and all these constants are assumed to be positive throughout the paper.

Using the estimates (7–10), we can define a comparison system $y' = f(y)$ for (1) from the above, where $f : \mathbb{R}_+^{12} \to \mathbb{R}^{12}$ is given by the right-hand sides of (7–10). Then it is easily seen that f is cooperative on $\mathbb{R}_+^{12}$; $Df(y) = \left(\partial f_i/\partial y_j\right)_{1\le i,j\le 12}$ is irreducible for any $y \in \mathbb{R}_+^{12}$; $f(0) = 0$ and $f_i(y) \ge 0$ for all $y \in \mathbb{R}_+^{12}$ with $y_i = 0, i = 1, 2, \ldots, n$. Furthermore, since all components of f are linear except that $f_{11}(y) = \delta\overline{d}_{10}y_{10} - \underline{d}_{11}y_{11} - \frac{\Delta_{11}}{N}y_{11}^2$, f is strictly sublinear, i.e., for any $\alpha \in (0, 1)$ and $y \in \operatorname{int}\mathbb{R}_+^{12}$, $f(\alpha y) > \alpha f(y)$. These properties mean that conditions (1–3) in Zhao and Jing (1996, Corollary 3.2) hold. Define

$$\begin{aligned} \mathcal{T}^* = &\left(\frac{\overline{p}f(0)}{\underline{d}_2 + \underline{\mu}_2}\right)\left(\frac{\overline{d}_2}{\underline{d}_3 + \underline{\mu}_3}\right)\left(\frac{\overline{d}_3}{\underline{d}_4 + \underline{\mu}_4}\right)\left(\frac{\overline{d}_{4r} + \overline{d}_{4b}}{\mu_5}\right)\left(\frac{\overline{d}_5}{\underline{d}_6 + \underline{\mu}_6}\right) \\ &\left(\frac{\overline{d}_6}{\underline{d}_7 + \underline{\mu}_7}\right)\left(\frac{\overline{d}_{7r} + \overline{d}_{7b}}{\mu_8}\right) \\ &\left(\frac{\overline{d}_8}{\underline{d}_9 + \underline{\mu}_9}\right)\left(\frac{\overline{d}_9}{\underline{d}_{10} + \underline{\mu}_{10}}\right)\left(\frac{\delta\overline{d}_{10}}{\underline{d}_{11}}\right)\left(\frac{\overline{d}_{11}}{\underline{d}_{12} + \underline{\mu}_{12}}\right)\left(\frac{\overline{d}_{12}}{\underline{\mu}_1}\right). \end{aligned}$$

One can check that $\mathcal{T}^* > 1$ if and only if the spectral bound of the linearization of f at $y = 0$ is positive (i.e., $s(Df(0)) > 0$). Then, by Corollary 3.2 of Zhao and Jing (1996), we have the following: (a) if $\mathcal{T}^* \le 1$, then $y = 0$ is a globally asymptotically stable equilibrium for the comparison system with respect to $\mathbb{R}_+^{12}$; (b) if $\mathcal{T}^* > 1$, then either (i) all solutions of the comparison system starting from $y \in \mathbb{R}_+^{12} \setminus \{0\}$ are unbounded, or (ii) the comparison system admits a positive equilibrium which is globally asymptotically stable with respect to $\mathbb{R}_+^{12} \setminus \{0\}$. Notice that if $\mathcal{T}^* > 1$, one can directly solve $f(y) = 0$ to find a positive equilibrium with all components expressed by the positive root of $0 = (\mathcal{T}^* - 1)y_{11} - \frac{\Delta_{11}}{\underline{d}_{11}N}y_{11}^2$, excluding (i) in case (b). Therefore, only cases (a) or (b) (ii) are possible, implying the boundedness of all solutions of the comparison system. By a comparison argument and the nonnegativity of solutions established above, we then conclude that every solution of (1) with nonnegative initial data is bounded for all $t \in [0, \infty)$. □

4 Dynamics of the Model System

It is easy to see that the system (1) has a tick-free (trivial) equilibrium. We notice that the tick dynamics in patch 1 is independent of the succeeding patches $i = 2, \ldots, N$, and generally, the tick dynamics on a patch j, $j \in \{2, 3, \ldots, N\}$, is independent from the succeeding patches k, $k \in \{j+1, \ldots, N\}$, but depends on that in the preceding patch $j-1$. Therefore, the complex system (1) over N patches is actually decoupled in a unidirectional sense. This simplifies the analysis of the model, allowing patch-wise analysis in a successive manner, as is done in the following subsections.

4.1 Dynamics in Patch 1

The system of tick population in source region (patch 1) is obtained by taking $i = 1$ in (1) and deleting the two delayed terms in the equations for $x'_{1,5b}(t)$ and $x'_{1,8b}(t)$. Denote this system by (P1), and let $x_1(t) = (x_{1,1}(t), \ldots, x_{1,12}(t))^T \in \mathbb{R}^{14}$ be the vector of all tick states in patch 1. The system (P1) obviously has a tick-free equilibrium (TFE), that is, the trivial equilibrium of (P1). The linearization of (P1) at this equilibrium can be written in the matrix form

$$\frac{\mathrm{d}x_1}{\mathrm{d}t} = (F(t) - V(t))x_1(t), \tag{11}$$

where $F(t) = (F_{ij}(t))_{14\times 14}$ is the so-called *production matrix* given by

$$F_{ij}(t) = \begin{cases} p(t)f(0), & i = 1, j = 2 \\ 0, & \text{otherwise,} \end{cases} \tag{12}$$

and $V(t) = (V_{ij}(t))_{14\times 14}$ is the so-called *progression matrix* with the diagonal entries being

$$\begin{array}{l} \mu_{1,1}(t);\, d_{1,2}(t) + \mu_{1,2}(t);\, d_{1,3}(t) + \mu_{1,3}(t);\, d_{1,4r}(t, R_1) \\ + d_{1,4b}(t, B_1(t)) + \mu_{1,4}(t); \\ d_{1,5r}(t) + \mu_{1,5r}(t, 0);\, m_{1,2}(t) + d_{1,5b}(t) + \mu_{1,5b}(t, 0);\, d_{1,6}(t) + \mu_{1,6}(t); \\ d_{1,7r}(t, R_1) + d_{1,7b}(t, B_1(t)) + \mu_{1,7}(t);\, d_{1,8r}(t) + \mu_{1,8r}(t, 0); \\ m_{1,2}(t) + d_{1,8b}(t) + \mu_{1,8b}(t, 0); \\ d_{1,9}(t) + \mu_{1,9}(t);\, d_{1,10}(t, D_1) + \mu_{1,10}(t);\, d_{1,11}(t) \\ + \mu_{1,11}(t, 0);\, d_{1,12}(t) + \mu_{1,12}(t), \end{array} \tag{13}$$

respectively, and the elements located on the first lower diagonal line being

$$\begin{array}{l} 0;\, -d_{1,2}(t);\, -d_{1,3}(t);\, -d_{1,4r}(t, R_1);\, 0;\, -d_{1,5b}(t);\, -d_{1,6}(t); \\ -d_{1,7r}(t, R_i);\, 0;\, -d_{1,8b}(t); \\ \quad -d_{1,9}(t);\, -\delta d_{1,10}(t, D_1);\, -d_{1,11}(t). \end{array}$$

Other nonzero elements of $V(t)$ are

$$V_{ij}(t) = \begin{cases} -d_{1,12}(t), & i = 1,\ j = 12, \\ -d_{1,4b}(t, B_1(t)), & i = 6,\ j = 4, \\ -d_{1,5r}(t), & i = 7,\ j = 5, \\ -d_{1,7b}(t, B_1(t)), & i = 10,\ j = 8, \\ -d_{1,8r}(t), & i = 11,\ j = 9, \end{cases}$$

and all the reminding elements are zeros in $V(t)$.

Following the approach developed in Bacaër and Guernaoui (2006), Wang and Zhao (2008), we can identify the basic reproduction ratio of the tick population in patch 1. Let C_ω denote the Banach space of continuous periodic function from $[0, \omega]$ to $\mathbb{R}^{14}$ equipped with the supremum norm. Define the evolution operator $Y(t, s)$ $(t \geq s)$ for the linear periodic system $y' = -V(t)y$, that is, $Y(t, s)$ satisfies

$$\frac{d}{dt}Y(t, s) = -V(t)Y(t, s) \quad t \geq s, \quad Y(s, s) = I,$$

where I is the 14×14 identity matrix. Then, for a given initial tick population distribution ϕ, $F(s)\phi(s)$ is the rate at which new ticks were produced by the initial ticks at time s, and $Y(t, s)F(s)\phi(s)$ is the distribution of those ticks who were newly produced at time s and still alive at time t. So the distribution of cumulative ticks at time t produced by all those initial ticks from the initial distribution $\phi(s)$ is given by

$$\psi(t) = \int_{-\infty}^{t} Y(t, s)F(s)\phi(s)\,ds = \int_{0}^{\infty} Y(t, t-a)F(t-a)\phi(t-a)\,da.$$

This naturally defines the linear operator $\mathcal{L} : C_\omega \to C_\omega$ by

$$(\mathcal{L}\phi)(t) = \int_{0}^{\infty} Y(t, t-a)F(t-a)\phi(t-a)\,da, \quad \forall t \in \mathbb{R}, \quad \phi(t) \in C_\omega.$$

which can be identified as the next-generation operator. The basic reproduction ratio of the tick population in patch 1 is thus defined as $\mathcal{R}_{10} = \rho(\mathcal{L})$, the spectral radius of $\mathcal{L}$. In terms of $\mathcal{R}_{10}$, we have the following results for (P1).

Theorem 4.1 *If the basic reproductive ratio $\mathcal{R}_{10} < 1$, then the TFE of (P1) is globally asymptotically stable; if $\mathcal{R}_{10} > 1$, then the TFE is unstable.*

Proof By Wang and Zhao (2008, Theorem 2.2), the TFE is locally asymptotically stable if $\mathcal{R}_{10} < 1$, and unstable if $\mathcal{R}_{10} > 1$. So, we only need to show that when $\mathcal{R}_{10} < 1$, the TFE is globally attractive.

Denote by $\Phi_{F-V}(t)$ the map of the linear ω-periodic system (11) and by $\rho(\Phi_{F-V}(\omega))$ the spectral radius of monodromy matrix $\Phi_{F-V}(\omega)$. Since $\mathcal{R}_{10} < 1$, we have $\rho(\Phi_{F-V}(\omega)) < 1$ (Wang and Zhao 2008, Theorem 2.2). By Lemma 6.1 in the "Appendix 2," $\Phi_{F-V}(t)$ is strongly positive for $t \geq 12\omega$. It then follows from Zhang

and Zhao (2008, Lemma 2.1) that there exists a positive 12ω-periodic function $h(t)$ such that

$$e^{\frac{1}{12\omega}t\ln(\rho(\Phi_{F-V}(12\omega)))}h(t) = e^{\frac{1}{12\omega}t\ln(\rho(\Phi_{F-V}(\omega)))^{12}}h(t) = e^{\frac{1}{\omega}t\ln(\rho(\Phi_{F-V}(\omega)))}h(t)$$

is a solution of (11). Since $\rho(\Phi_{F-V}(\omega)) < 1$, $e^{\frac{1}{\omega}t\ln(\rho(\Phi_{F-V}(\omega)))}h(t) \to 0$ as $t \to \infty$. Now, for any nonnegative initial value x_1^0, there is a sufficiently large positive constant M such that $x_1^0 \le Mh(0)$. Note that due to the monotone properties of the functions $f(\cdot)$, $\mu_{i,5r}(t,\cdot)$, $\mu_{i,5b}(t,\cdot)$, $\mu_{i,8r}(t,\cdot)$, $\mu_{i,8b}(t,\cdot)$ and $\mu_{i,11}(t,\cdot)$, we can easily see that (P1) is actually controlled from above by the cooperative linear system (11). By the comparison principle, we then have $0 \le x_1(t,x_1^0) \le Me^{\frac{1}{\omega}t\ln(\rho(\Phi_{F-V}(\omega)))}h(t)$. Therefore, we obtain $x_1(t,x_1^0) \to 0$ as $t \to \infty$, proving the global attractivity of the TFE for (P1) and thereby completing the proof of the theorem. □

The next theorem shows that the ticks will be established in the sense of uniform persistence, provided that $\mathcal{R}_{10} > 1$.

Theorem 4.2 *If the basic reproduction ratio $\mathcal{R}_{10} > 1$, then there exists an $\epsilon > 0$ such that every solution $x_1(t,x_1^0)$ of (P1) with initial value $x_1^0 \in \mathbb{R}_+^{14} \setminus \{0\}$ satisfies*

$$\liminf_{t\to\infty} x_{1,j}(t,x_1^0) > \epsilon, \ \textit{for} \ \ j \in \mathcal{C},$$

implying that the tick population establishes in patch 1; moreover, (P1) admits a positive periodic solution.

Proof Proposition 3.1 implies that system (P1) is point dissipative. Let $\Psi(t)$ be the solution map to system (P1), that is,

$$\Psi(t)(x_1^0) = x_1(t,x_1^0), \ \forall x_1^0 \in \mathbb{R}_+^{14},$$

where $x_1(t,x_1^0)$ is the unique solution of (P1) with $x_1(0,x_1^0) = x_1^0$. Let $P : \mathbb{R}_+^{14} \to \mathbb{R}_+^{14}$ be the Poincaré map to system (P1), that is,

$$P(x_1^0) = \Psi(\omega)(x_1^0), \ \forall x_1^0 \in \mathbb{R}_+^{14}.$$

Define $Y = \mathbb{R}_+^{14}$, $Y_0 = Int\mathbb{R}_+^{14} = \{x_1 \in \mathbb{R}_+^{14} : x_{1,j} > 0, j \in \mathcal{C}\}$. Then $\partial Y_0 := Y \setminus Y_0 = \{x_1 \in \mathbb{R}_+^{14} : \Pi_{j\in\mathcal{C}} x_{1,j} = 0\}$. We first prove that P is uniformly persistent with respect to $(Y_0, \partial Y_0)$. By the form of (P1), it is easy to see that both Y and Y_0 are positively invariant. Clearly, ∂Y_0 is relatively closed in Y.

Set $M_\partial = \{x_1 \in \mathbb{R}_+^{14} : P^m(x_1) \in \partial Y_0, \forall m > 0\}$, and then it is easy to see that $M_\partial = \{0\}$. Since $\mathcal{R}_{10} > 1$, it then follows from Wang and Zhao (2008, Theorem 2.2) that $\rho(\Phi_{F-V}(\omega)) > 1$. By the continuity of $f(\cdot)$, $\mu_{1,5r}(t,\cdot)$, $\mu_{1,5b}(t,\cdot)$, $\mu_{1,8r}(t,\cdot)$, $\mu_{1,8b}(t,\cdot)$ and $\mu_{1,11}(t,\cdot)$, we know that for sufficiently small $\delta > 0$, we also have $\rho(\Phi_{F_\delta - V_\delta}(\omega)) > 1$, where F_δ is the matrix resulted from replacing $f(0)$ by $f(\delta)$ in F and V_δ is the matrix obtained by replacing $\mu_{1,5r}(t,0)$, $\mu_{1,5b}(t,0)$, $\mu_{1,8r}(t,0)$, $\mu_{1,8b}(t,0)$ and $\mu_{1,11}(t,0)$, respectively, by

$\mu_{1,5r}(t,\delta)$, $\mu_{1,5b}(t,\delta)$, $\mu_{1,8r}(t,\delta)$, $\mu_{1,8b}(t,\delta)$ and $\mu_{1,11}(t,\delta)$ in V. For such a $\delta > 0$, by the continuity of solutions with respect to the initial values, there is an $\eta > 0$ such that $||x_1(t,x_1^0)|| = ||x_1(t,x_1^0) - 0|| = ||x_1(t,x_1^0) - x_1(t,0)|| < \delta$ for $t \in [0,\omega]$, provided that $||x_1^0|| < \eta$.

Claim $\limsup_{n\to\infty} \|P^n(x_1^0)\| \geq \eta$ for all $x_1^0 \in Y_0$.

Suppose, for the sake of contradiction, that $\limsup_{n\to\infty} \|P^n x_1^0\| < \eta$ for some $x_1^0 \in Y_0$. Without loss of generality, we can assume $\|P^n x_1^0\| < \eta$ for all $n \geq 0$. It then follows that

$$||x_1(t, P^n x_1^0)|| < \delta \quad \text{for all} \quad n \geq 0,\ t \in [0,\omega]$$

Now, for any $t > 0$, it can be written as $t = m\omega + t'$ where $m \geq 0$ is an integer and $t' \in [0,\omega]$, and therefore, we indeed have

$$||x_1(t,x_1^0)|| = ||x_1(t', P^m x_1^0)|| < \delta, \quad t' \in [0,\omega]. \tag{14}$$

By the estimate (14) and the monotone properties of $f(\cdot)$, $\mu_{1,5r}(t,\cdot)$, $\mu_{1,5b}(t,\cdot)$, $\mu_{1,8r}(t,\cdot)$, $\mu_{1,8b}(t,\cdot)$ and $\mu_{1,11}(t,\cdot)$, we observe that the linear system

$$\frac{\mathrm{d}x_1}{\mathrm{d}t} = (F_\delta(t) - V_\delta(t))x_1(t), \tag{15}$$

is a comparison system for (1) from below which is cooperative. By Zhang and Zhao (2008, Lemma 2.1), there exists a positive, ω-periodic function $g(t) \in \mathbb{R}^{14}_+$ such that $e^{\nu t}g(t)$ is a solution of (15), where $\nu = \frac{1}{\omega}\ln(\rho(\Phi_{F_\delta - V_\delta}(\omega))) > 0$. Choose $\sigma > 0$ sufficiently small such that $x_1^0 \geq \sigma g(0)$. Then, by the comparison principle, we have

$$x_1(t,x_1^0) \geq \sigma e^{\nu t} g(t) \quad \text{for } t \geq 0$$

which contradicts (14) since $\nu > 0$. The contradiction proves the claim.

Note that every orbit in M_∂ approaches $\{0\}$, implying that $\{0\}$ is acyclic in M_∂. It then follows from Zhao (2003, Theorem 3.1.1) that the solutions of system (P1) are actually uniformly persistent with respect to $(Y_0, \partial Y_0)$, that is, there exists an $\epsilon > 0$ such that any solution $x_1(t,x_1^0)$ of system (P1) with initial value $x_1^0 \in \mathbb{R}^{14}_+$ with $x_1^0 \neq 0$ satisfies

$$\liminf_{t\to\infty} x_{1,j}(t,x_1^0) > \epsilon, \quad \text{for all} \quad j \in \mathcal{C}.$$

Furthermore, Zhao (2003, Theorem 1.3.6) implies that the Poincaré map P has a fixed point $x_1^* \in Y_0$, implying that $x_1(t,x_1^*)$, the solution through x_1^*, is a positive periodic solution. □

We note that in the absence of bird migration, the system (Pi) at patch i is nothing but an ordinary differential equation system with periodic coefficients. Such a system consists of 12 equations presenting the tick reproduction cycle in the local environment, and the associated basic reproduction ratio and the threshold dynamics are also

determined by the same statement as mentioned above. In what follows, we denote by $\mathcal{R}_{i0}^{\text{loc}}$ the basic reproduction ratio of the tick population in patch i in the absence of bird migration, that is, when the patches are disconnected.

4.2 Tick Dynamics at Patch 2 (P2)

4.2.1 The Case of $\mathcal{R}_{10} < 1$

When $\mathcal{R}_{10} < 1$, every solution of system (P1) approaches the trivial equilibrium, and the ticks will go to extinction in patch 1. This indicates that the local habitat and host abundance do not favor the survival of *I. scapularis* in patch 1. As a result, seasonal bird migration in spring cannot offer a sustainable source of ticks for the succeeding patch. Indeed, the limiting system for the tick population in patch 2 is nothing but (1) with $i = 2$ and with the two delayed terms removed. In other words, the tick dynamics in patch 2 only depends on the local reproduction, development and death, as well as emigration to patch 3 by migratory birds. This system, denoting it by (P2), is exactly the same as (P1) except for the subindex which is 2 rather than 1 now. Therefore, we can define the basic reproduction ratio for patch 2 in exactly the same way as for patch 1, denoting it by $\mathcal{R}_{20}$. Then the same conclusions for patch 1 also hold for patch 2, in terms of $\mathcal{R}_{20}$ now, as stated in the next theorem.

Theorem 4.3 *Assume that $\mathcal{R}_{10} < 1$. Then,*

(i) if $\mathcal{R}_{20} < 1$, then the trivial solution of system (P2) is globally asymptotically stable, and thus, the ticks will ultimately die out in both patches 1 and 2.

(2) If $\mathcal{R}_{20} > 1$, then there exists at least one positive periodic solution for (P2); more specifically, tick population persists in patch 2 due to local suitability for tick establishment, while tick population cannot establish at patch 1.

4.2.2 The Case of $\mathcal{R}_{10} > 1$

In this case, (P1) has a positive periodic solution $x_1^*(t)$ by Theorem 4.2. Substituting $x_{1,5b}^*(t)$ and $x_{1,8b}^*(t)$ into (1) with $i = 2$ for the two delayed terms $x_{1,5b}(t-\tau_1)$ and $x_{1,8b}(t-\tau_1)$ results in the following new periodic system for the tick population in patch 2:

$$
\begin{aligned}
x_{2,1}'(t) &= d_{2,12}(t)x_{2,12}(t) - \mu_{2,1}(t)x_{2,1}(t),\\
x_{2,2}'(t) &= p(t)f(x_{2,11}(t))x_{2,1}(t) - d_{2,2}(t)x_{2,2}(t) - \mu_{2,2}(t)x_{2,2}(t),\\
x_{2,3}'(t) &= d_{2,2}(t)x_{2,2}(t) - d_{2,3}(t)x_{2,3}(t) - \mu_{2,3}(t)x_{2,3}(t),\\
x_{2,4}'(t) &= d_{2,3}(t)x_{2,3}(t) - d_{2,4r}(t, R_2)x_{2,4}(t)\\
&\quad -d_{2,4b}(t, B_2(t))x_{2,4}(t) - \mu_{2,4}(t)x_{2,4}(t),\\
x_{2,5r}'(t) &= d_{2,4r}(t, R_2)x_{2,4}(t) - d_{2,5r}(t)x_{2,5r}(t) - \mu_{2,5r}(t, x_{2,5r}(t))x_{2,5r}(t),\\
x_{2,5b}'(t) &= d_{2,4b}(t, B_2(t))x_{2,4}(t) + \boxed{\alpha_{1,2}^l(t)m_{1,2}(t-\tau_1)x_{1,5b}^*(t-\tau_1)}\\
&\quad - m_{2,3}(t)x_{2,5b}(t) - d_{2,5b}(t)x_{2,5b}(t) - \mu_{2,5b}(t, x_{2,5b}(t))x_{2,5b}(t),
\end{aligned}
$$

$$
\begin{aligned}
x'_{2,6}(t) &= d_{2,5r}(t)x_{2,5r}(t) + d_{2,5b}(t)x_{2,5b}(t) - d_{2,6}(t)x_{2,6}(t) - \mu_{2,6}(t)x_{2,6}(t),\\
x'_{2,7}(t) &= d_{2,6}(t)x_{2,6}(t) - d_{2,7r}(t, R_2)x_{2,7}(t)\\
&\quad -d_{2,7b}(t, B_2(t))x_{2,7}(t) - \mu_{2,7}(t)x_{2,7}(t),\\
x'_{2,8r}(t) &= d_{2,7r}(t, R_2)x_{2,7}(t) - d_{2,8r}(t)x_{2,8r}(t) - \mu_{2,8r}(t, x_{2,8r}(t))x_{2,8r}(t),\\
x'_{2,8b}(t) &= d_{2,7b}(t, B_2(t))x_{2,7}(t) + \boxed{\alpha^n_{1,2}(t)m_{1,2}(t-\tau_1)x^*_{1,8b}(t-\tau_1)}\\
&\quad - m_{2,3}(t)x_{2,8b}(t) - d_{2,8b}(t)x_{2,8b}(t) - \mu_{2,8b}(t, x_{2,8b}(t))x_{2,8b}(t),\\
x'_{2,9}(t) &= d_{2,8r}(t)x_{2,8r}(t) + d_{2,8b}(t)x_{2,8b}(t) - d_{2,9}(t)x_{2,9}(t) - \mu_{2,9}(t)x_{2,9}(t),\\
x'_{2,10}(t) &= d_{2,9}(t)x_{2,9}(t) - d_{2,10}(t, D_2)x_{2,10}(t) - \mu_{2,10}(t)x_{2,10}(t),\\
x'_{2,11}(t) &= \delta d_{2,10}(t, D_2)x_{2,10}(t) - d_{2,11}(t)x_{2,11}(t) - \mu_{2,11}(t, x_{2,11}(t))x_{2,11}(t),\\
x'_{2,12}(t) &= d_{2,11}(t)x_{2,11}(t) - d_{2,12}(t)x_{2,12}(t) - \mu_{2,12}(t)x_{2,12}(t).
\end{aligned} \tag{16}
$$

System (16) is controlled from below by (P2) described in Sect. 4.2.1, that is, the system obtained by dropping the two delayed terms in (16). By the results in Sect. 4.1 for patch 1 (need to replace subindex 1 by 2), this system (P2) has the basic reproduction ratio $\mathcal{R}_{20}$, and if $\mathcal{R}_{20} > 1$, then (P2) is uniformly persistent, and by the comparison principle, so is (16) and as a consequence, (16) also has positive periodic solution (Zhao 2003, Theorem 1.3.6)

It is interesting to ask what happens if $\mathcal{R}_{20} < 1$. In this subsection, we show that even if $\mathcal{R}_{20} < 1$, due to the contribution from patch 1, the tick population can also remain persistent in the sense that the system (16) also admits a positive periodic solution.

Theorem 4.4 *Assume that $\mathcal{R}_{10} > 1$. Then system (16) is uniformly persistent and admits a positive periodic solution, regardless of whether $\mathcal{R}_{20} > 1$ or $\mathcal{R}_{20} < 1$.*

Proof Let $\underline{\mu}^0_{2,j} = \min_{t\in[0,\omega]} \mu_{2,j}(t, 0)$ for $j = 5r, 5b, 8r, 8b$ and $D_{11} = \min_{t\in[0,\omega]} \frac{\partial \mu_{2,11}(t,0)}{\partial x_{2,11}}$. Since $f(\cdot)$ is a decreasing function and all density-dependent death rates are increasing functions with respect to their state variables, the system (16) is controlled from above by the following autonomous and cooperative system:

$$
\begin{aligned}
u'_{2,1}(t) &= \bar{d}_{2,12}u_{2,12}(t) - \underline{\mu}_{2,1}u_{2,1}(t),\\
u'_{2,2}(t) &= \bar{p}f(0)u_{2,1}(t) - \underline{\mu}_{2,2}u_{2,2}(t),\\
u'_{2,3}(t) &= \bar{d}_{2,2}u_{2,2}(t) - \underline{\mu}_{2,3}u_{2,3}(t),\\
u'_{2,4}(t) &= \bar{d}_{2,3}u_{2,3}(t) - \underline{\mu}_{2,4}u_{2,4}(t),\\
u'_{2,5r}(t) &= \bar{d}_{2,4r}u_{2,4}(t) - \underline{\mu}^0_{2,5r}u_{2,5r}(t),\\
u'_{2,5b}(t) &= \bar{d}_{2,4b}u_{2,4}(t) + \boxed{\bar{\alpha}^l_{1,2}\bar{m}_{1,2}\bar{x}^*_{1,5b}} - \underline{\mu}^0_{2,5b}u_{2,5b}(t),\\
u'_{2,6}(t) &= \bar{d}_{2,5}[u_{2,5r}(t) + u_{2,5b}(t)] - \underline{\mu}_{2,6}u_{2,6}(t),\\
u'_{2,7}(t) &= \bar{d}_{2,6}u_{2,6}(t) - \underline{\mu}_{2,7}u_{2,7}(t),
\end{aligned} \tag{17}
$$

$$
\begin{aligned}
u'_{2,8r}(t) &= \bar{d}_{2,7r}u_{2,7}(t) - \underline{\mu}^0_{2,8r}u_{2,8r}(t),\\
u'_{2,8b}(t) &= \bar{d}_{2,7b}u_{2,7}(t) + \boxed{\bar{\alpha}^n_{1,2}\bar{m}_{1,2}\bar{x}^*_{1,8b}} - \underline{\mu}^0_{2,8b}u_{2,8b}(t),\\
u'_{2,9}(t) &= \bar{d}_{2,8}[u_{2,8r}(t) + u_{2,8b}(t)] - \underline{\mu}_{2,9}u_{2,9}(t),\\
u'_{2,10}(t) &= \bar{d}_{2,9}u_{2,9}(t) - \underline{\mu}_{2,10}u_{2,10}(t),\\
u'_{2,11}(t) &= \delta\bar{d}_{2,10}u_{2,10}(t) - \boxed{D_{11}u^2_{2,11}(t)},\\
u'_{2,12}(t) &= \bar{d}_{2,11}u_{2,11}(t) - \underline{\mu}_{2,12}u_{2,12}(t).
\end{aligned}
$$

By setting the terms on the right sides of system (17) to zeros, we are led to a quadratic function

$$a_1u^2_{2,11} - a_2u_{2,11} - a_3 = 0, \tag{18}$$

where a_1, a_2 and a_3 are some positive constants. Equation (18) admits a unique positive root

$$u^*_{2,11} = \frac{a_2 + \sqrt{a_2^2 + 4a_1a_3}}{2a_1} > 0,$$

implying that the system (17) has a unique positive equilibrium, denoting by $u^*_2 \in \mathbb{R}^{14}_+$ with $u^*_2 \gg 0$. Since system (17) is strongly monotone, by a similar argument as that in the proof as Heffernan et al. (2014, Lemma 3.1), we conclude that the positive equilibrium u^*_2 is globally attractive in $\mathbb{R}^{14}_+$.

By the comparison principle, we then have $\limsup_{t\to\infty} x_{2,11}(t, x^0_2) \le u^*_{2,11}$. Thus, for every $\epsilon > 0$, there exists some sufficiently large $t_1 > 0$ such that

$$x_{2,11}(t, x^0_2) \le u^*_{2,11} + \epsilon \quad \text{for all } t \ge t_1. \tag{19}$$

From the second equation in (16) and inequality (19), we then have

$$
\begin{aligned}
x'_{2,2}(t) &= p(t)f(x_{2,11}(t, x^0_2))x_{2,1}(t) - d_{2,2}(t)x_{2,2}(t) - \mu_{2,2}(t)x_{2,2}(t)\\
&\ge p(t)f(u^*_{2,11} + \epsilon)x_{2,1}(t) - d_{2,2}(t)x_{2,2}(t) - \mu_{2,2}(t)x_{2,2}(t), \quad t \ge t_1.
\end{aligned}
$$

Therefore, replacing $f(x_{2,11}(t))$ by $f(u^*_{2,11} + \epsilon)$ in (16) results in a new system, denoted by (MS), which controls (16) from below. By arguments similar to that in the proof of Lemma (6.1) in "Appendix 2," it is easy to see that system (MS) is eventually strongly monotone (e.g., strongly monotone for $t \ge 12\omega$). By using the same arguments as in that of (Heffernan et al. 2014, Theorem 3.2), that is, by showing that $[0, ku^*_2]$ is positively invariant for the system (MS) when k is large and by constructing two positive sequences and applying the squeeze principle, we conclude that system (MS) admits a positive ω-periodic solution $\hat{x}^*_2(t) \gg 0$ which is globally attractive. Let $\varepsilon = \min\{\inf \hat{x}^*_{2,j}(t), \ \ j \in \mathcal{C}\}$. Then by the comparison principle, every positive

solution $x_2(t)$ of system (16) satisfies

$$\liminf_{t\to\infty} x_{2,j}(t) \geq \varepsilon, \quad j \in \mathcal{C}. \tag{20}$$

That is, (16) is uniformly persistent, and by Zhao (2003, Theorem 1.3.6), (16) admits a positive periodic solution. The proof of Theorem 4.4 is completed. □

Continuing the same process to all other patches, we summarize our conclusions over N patches as below.

Step 1 Calculate $\mathcal{R}_{10}$. If $\mathcal{R}_{10} > 1$, each patch allows to have a positive solution and tick population is endemic at each patch due to the transportation of the migratory birds; if $\mathcal{R}_{10} < 1$, trivial solution is globally asymptotically stable and tick population is free at patch 1.

Step 2 Calculate $\mathcal{R}_{k0}$ for $k = 2, \ldots, i+1$ until $\mathcal{R}_{(i+1)0} > 1$ for some i, and then tick population is free at patches $k = 1, \ldots, i$, which will be persistent in the remaining patches starting from patch $i+1$, admitting a positive periodic solution in each of the patches $i+1, \cdots, N$.

We note that the first endemic patch of tick population becomes a source to spread the tick population to all succeeding patches via bird migration. Similar phenomenon but not for a periodic system was found in a multi-patch epidemic model due to population transportation in Nakata and Röst (2015).

5 Numerical Simulations

In this section, we carry out some numerical simulations to demonstrate the effects of bird migration on tick populations. For simplicity, we consider the source region (patch 1) and the subsequent stopover (patch 2) during spring migration to examine how the tick population is affected by bird migration from the source region. To this end, we first need to estimate the populations of the migration birds at the two patches and denote by $B_1(t)$ and $B_2(t)$, respectively.

To the best of our knowledge, the immigration of migratory birds into the source region (patch 1) is fairly more complicated than simply migrating back southward, since they undergo not only a couple of stopovers during fall migration, but also winter feeding (Bourouiba et al. 2010). These factors lead to considerable variation in the number of birds arriving (indirectly) at patch 1 from patch N. Note that patch N is assumed to be the one in which birds start fall migration. Meanwhile, the distribution of winter feeding of these Lyme-tick carrying birds (e.g., American robins) is very wide; moreover, landscapes and food resources at wintering sites also change the bird migration routes (Bird Life international 2013; Robin Migration Study 2015). Consequently, the influx of birds at patch 1 is not merely determined by the number of migratory birds at patch N. For simplicity or numeric simulations, we assume that the influx of birds at patch 1 is given by a constant recruitment rate r_0 during the spring migration window $[t_{\text{start}}, t_{\text{end}}] \subset [0, 365]$, while they die at a rate μ_1^b and depart from patch 1 at a migration rate $m_{1,2}(t)$. In patch 2, birds arrive at a rate

$e^{-\mu_{1,2}^b \tau_1} m_{1,2}(t-\tau_1) B_1(t-\tau_1)$ after flying time τ_1 from patch 1, die at a death rate μ_2^b during their stay in patch 2 and will leave patch 2 at a migration rate $m_{2,3}(t)$, where $m_{2,3}(t)$ is the migration rate of birds from patch 2 to the following patch 3. Therefore, the populations of birds in the first two patches can be calculated from the following equations

$$\begin{cases} B_1'(t) = r(t) - (m_{1,2}(t) + \mu_1^b) B_1(t) \\ B_2'(t) = e^{-\mu_{1,2}^b \tau_1} m_{1,2}(t-\tau_1) B_1(t-\tau_1) - (m_{2,3}(t) + \mu_2^b) B_2(t) \end{cases} \tag{21}$$

where

$$r(t) = \begin{cases} r_0, & t \in [t_{\text{start}}, t_{\text{end}}], \\ 0, & \text{otherwise}, \end{cases}$$

and

$$m_{1,2}(t) = \begin{cases} m_{12}, & t \in [t_{\text{start}}, t_{\text{end}}], \\ 0, & \text{otherwise}, \end{cases} \qquad m_{2,3}(t) = \begin{cases} m_{23}, & t \in [t_{\text{start}} + \tau_1, t_{\text{end}} + \tau_1], \\ 0, & \text{otherwise}. \end{cases}$$

Following Bourouiba et al. (2010), we assume that during the migration window, 99.99 % of the birds that arrive at a patch will have departed the patch at the end of the season, meaning that only 0.01 % remains in the patch at the end of the season. For patch 1, this translates to

$$e^{-(m_{12}+\mu_1^b)(t_{\text{end}}-t_{\text{start}})} = 0.01\,\% = 10^{-4},$$

i.e., $m_{12} = 4 \ln 10/(t_{\text{end}} - t_{\text{start}}) - \mu_1^b$. Similarly, $m_{23} = 4 \ln 10/(t_{\text{end}} - t_{\text{start}}) - \mu_2^b$.

Adopting the spring migration time window $[t_{\text{start}}, t_{\text{end}}]$=[March 1, June 30] (see Ogden et al. 2008), and the parameter values as $r_0 = 300/\text{day}$ and $\tau_1 = 2\,\text{days}$, $\mu_1^b = \mu_2^b = 0.03/\text{day}$, $\mu_{1,2}^b = 0.0014/\text{day}$, and accordingly $m_{12} = 0.0741/\text{day}$ and $m_{23} = 0.0741/\text{day}$. With the above, the number of bird population at patches 1 and 2 can be solved based on (21) to display the seasonal populations of the migratory birds which will be used in the following simulations.

5.1 The Dependence of $\mathcal{R}_{10}$ on Some Migratory Parameters

As in most models, the basic reproduction ratio in each patch in our model cannot be obtained explicitly. However, with the above preparation, we can use the dichotomy method developed in Bacaër (2007), Wang and Zhao (2008) to numerically compute these ratios. The main idea is that after writing the linearization of the periodic model system at the tick-extinction equilibrium in the form $\mathrm{d}X/\mathrm{d}t = (F(t)/\mathcal{R} - V(t))X(t)$, the value of $\mathcal{R}$ that allows this linear system to have the dominant Floquet multiplier equal to 1 gives the basic reproduction ratio.

We start with patch 1 and use parameters in Tables 2 and 3 for the constant parameters, and in the mean time, we adopt the periodic coefficients in Wu et al. (2013) with the mean monthly temperatures in the order from January to December being [−7.70; −7.39; −2.64; 4.21; 10.18; 15.20; 18.60; 18.39; 14.39; 8.37; 2.60; −3.72].

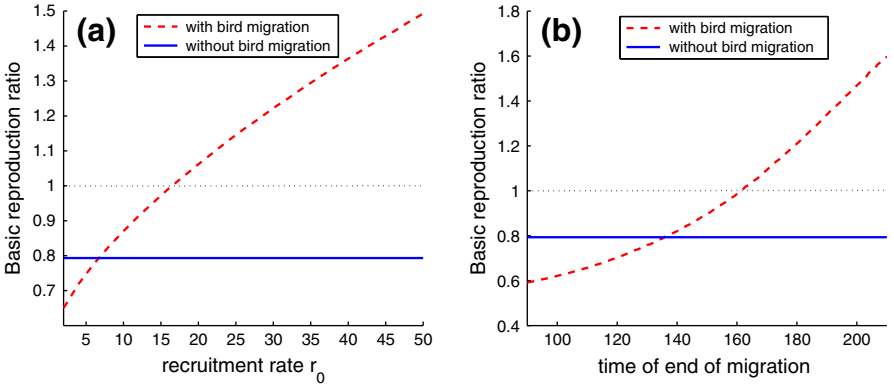

Fig. 2 Dependence of the basic reproduction ratios $\mathcal{R}_{10}$ and $\mathcal{R}_{10}^{\text{loc}}$ on **a** the bird recruitment r_0 with $t_{\text{start}} = 60$ and $t_{\text{end}} = 181$, and **b** on the migration ending time t_{end} with $r_0 = 30$ and $t_{\text{start}} = 60$

Then, implementing the algorithm based on the aforementioned dichotomy method, we obtain the numeric plots of $\mathcal{R}_{10}$ and $\mathcal{R}_{10}^{\text{loc}}$ with respect to r_0 and the t_{end}, respectively, as shown in Fig. 2. From Fig. 2a, it is interesting to note that there is a critical value for r_0, below which $\mathcal{R}_{10} < \mathcal{R}_{10}^{\text{loc}}$, and above which $\mathcal{R}_{10} > \mathcal{R}_{10}^{\text{loc}}$. Figure 2b reveals a similar phenomenon with respect to the ending time t_{end}. Note that although $\mathcal{R}_{10}$ is increasing in both r_0 and t_{end}, $\mathcal{R}_{10}$ is concave down in r_0 but concave up in t_{end}, meaning that $\mathcal{R}_{10}$ is more sensitive to smaller r_0 and larger t_{end} than to larger r_0 and smaller t_{end}; in both cases, $\mathcal{R}_{10}$ can achieve a value larger than 1 for large r_0 and t_{end}, although $\mathcal{R}_{10}^{\text{loc}} = 0.7931 < 1$.

5.2 Subpopulations of Ticks in Patch 2

For patch 2, we can do the same thing for $\mathcal{R}_{20}$ and $\mathcal{R}_{20}^{\text{loc}}$ and obtain similar observations. We will not pursue along this line here; instead, we will explore the impact of migration birds on the subpopulations of ticks in patch 2 in the case of $\mathcal{R}_{10} > 1$. In what follows, we still use the same bird populations $B_1(t)$ and $B_2(t)$ as described above and keep the same values of constant parameters as in Tables 2 and 3. Then taking $r_0 = 300/day$, $t_{\text{start}} = 60$ and $t_{\text{end}} = 181$ and using the mean monthly temperatures from January to December $[-4.05; -3.02; 1.67; 7.69; 13.99; 19.46; 22.12; 21.46; 17.67; 11.26; 5.28; -0.89]$ to estimate those periodic coefficients, we numerically obtain $\mathcal{R}_{10} = 8.5422$ and simulate the subpopulations in patch 1 as plotted in Fig. 3. In the rest of these subsections, these tick subpopulations in patch 1 in a 1-year period will be used to numerically calculate the basic reproduction ratio $\mathcal{R}_{20}$ and $\mathcal{R}_{20}^{\text{loc}}$ and find the tick subpopulations in patch 2.

For patch 2, we first use the mean monthly temperatures from January to December $[-9.75; -8.23; -2.08; 6.03; 13.30; 18.35; 20.79; 19.64; 14.98; 8.25; 2.06; -5.66]$ to estimate the associated periodic coefficients, by which we numerically obtain $\mathcal{R}_{20}^{\text{loc}} = 1.8338$ by the aforementioned numeric method. This implies that in the absence of migratory birds, tick populations can persist. Now, using the tick subpopulations in

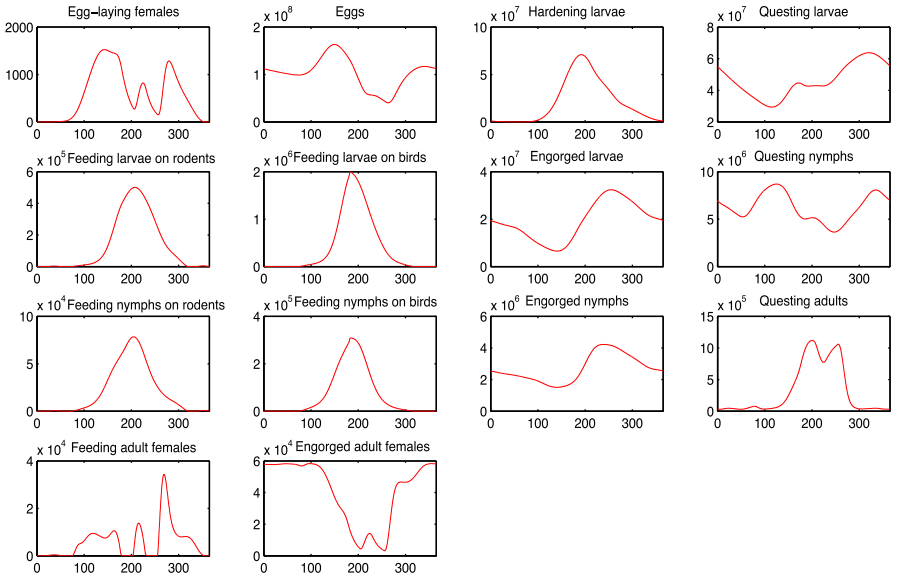

Fig. 3 Subpopulations at a rich source region (patch 1) with $\mathcal{R}_{10} = 8.5422$ as described in the text

patch 1 in a 1-year period as shown in Fig. 3, we obtain the numeric simulations of the subpopulations in patch 2 for some selected stages, as illustrated in Fig. 4. In this figure, the solid curves measured by the vertical axes on the left present the subpopulations of ticks *in the absence* of bird migration, while the dash curves measured by the vertical axes on the right account for the subpopulations of the ticks *in the presence* of migratory birds which are much higher than the solid curves. This clearly shows the positive effect of migration birds on the tick populations in patch 2.

Again for patch 2, if we choose the mean monthly temperatures from January to December as $[-13.42; -11.41; -5.07; 3.21; 10.82; 15.98; 18.39; 17.20; 12.29; 5.59; -1.07; -9.34]$, we accordingly obtain $\mathcal{R}_{20}^{\text{loc}} = 0.5683 < 1$, meaning that patch 2 is a poor environment for the ticks: In the absence of the migration of birds, the ticks will go to extinction in this patch. Now, using the tick subpopulations in patch 1 in a 1-year period as shown in Fig. 3, we can numerically solve the model for the subpopulations in patch 2, as illustrated in Fig. 5, which shows that the tick subpopulations form a self-reproduction cycle from the scratch with the help of bird migration. This indicates that migratory birds are capable of helping the ticks to establish in a poor region where the environment is not good enough to support the establishment of the tick population.

6 Conclusion and Discussion

In this study, we have developed a general framework which integrates the local landscape for the ticks and the distribution of the ticks through the migratory birds during spring. The model turns out to be a patch-based periodic system of delay differential equations with multiple delays. The delays account for the flying times

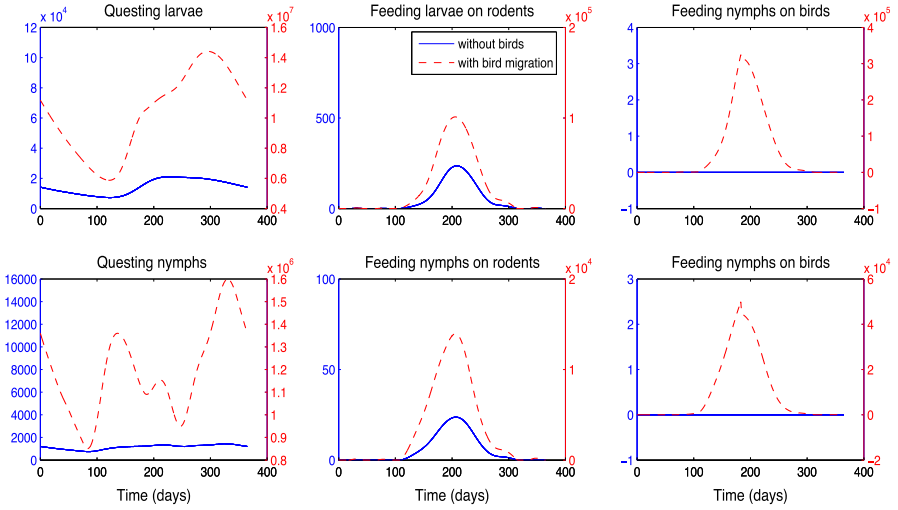

Fig. 4 Subpopulations of selected tick stages in patch 2 with/without the help of migratory birds when this patch is a "good" one for the ticks: $\mathcal{R}_{20}^{\mathrm{loc}} = 1.8338 > 1$

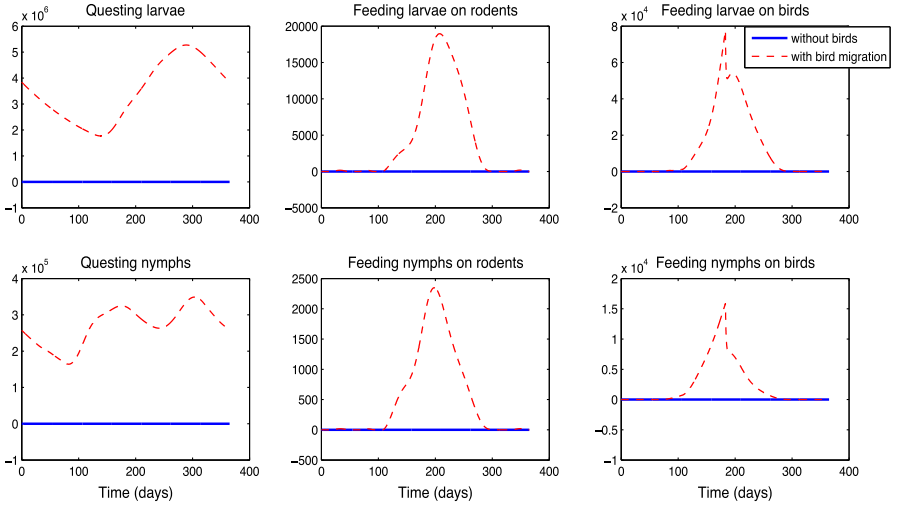

Fig. 5 Subpopulations of selected tick stages in patch 2 with/without the help of migratory birds when this patch is a "poor" one for the ticks: $\mathcal{R}_{20}^{\mathrm{loc}} = 0.5683 < 1$

of birds from preceding patches to succeeding patches on the migratory route, and the periodic coefficients are chosen to reflect the local suitability depending on local climate (e.g., temperature) changes. Since the ticks are barely active in the late fall when the birds start migrating back, the long-distance dispersal of the ticks is unidirectional from south to north, and accordingly, the full system (1) is indeed decoupled into subsystems, in each of which the tick population dynamics depends on the information of the current and preceding patch rather than the succeeding patch. This allows us

to investigate the tick dynamics in all patches in a successive way, starting from the southern most patch (patch 1). Taking advantage of this and with the help of the developed theory for the monotone dynamical systems in a periodic setting, we are able to derive the basic reproduction ratio for each patch to characterize the long-term behavior of the tick population (Smith 1995; Wang and Zhao 2008; Zhao 2003) in the patch. Not surprisingly, the dynamics of the tick population in a patch affects that in all succeeding patches due to the migratory birds. What is significant is that this work provides a framework for quantitatively exploring such an impact, particularly for numerical explorations.

We have found that migratory birds during spring migration play a crucial role in the range expansion of *I. scapularis* by spreading the ticks to a long distance. The migratory birds have the potential to transport Lyme-ticks to more northerly regions, provided that the resource region is sufficiently rich in ticks (i.e., $\mathcal{R}_{10} > 1$). However, the risk of Lyme disease to public health in the northern regions (patch 2 in our simulations) is heavily dependent on the local environment in the sense that (1) if the tick population is already endemic in a patch, the risk has been observed to be increased (Fig. 4); (2) if a region is a "poor one" in the sense that the ticks cannot be established locally, then the tick population could be present by the aid of migratory birds, thus bringing the risk to the region (Fig. 5). The study in Heffernan et al. (2014) only considered a one-patch model, rather than multiple patches as in our current study, and directly assumed that some ticks are carried by migratory birds into the patch. In contrast to Heffernan et al. (2014), here we have derived in detail a multi-patch model in terms of the specific life cycle of the Lyme-tick population, the heterogeneous landscape and the spring bird migration; thus, the corresponding model is more realistic, the system is much larger, and the mathematical analysis of the model system is much more challenging. Despite this, we are able to examine the establishment of tick population in a way of multiple successive patches. Importantly, we have found that the spring bird migration not only can have a positive effect on the establishment of the Lyme-tick population as observed in Heffernan et al. (2014), but can also have a negative impact, depending on its level. This is demonstrated in Fig. 2, where a smaller influx of birds or shorter migration window could lead to a value of $\mathcal{R}_{10}$ lower than $\mathcal{R}_0^{\text{loc}}$, while larger influx rate results in a value of $\mathcal{R}_{10}$ larger than $\mathcal{R}_0^{\text{loc}}$. The negative effect seems to be counterintuitive; however, this can be explained by noticing that i) the numeric result in Fig. 2 is obtained with the out-flux of birds fixed, and ii) ticks are carried in and out by birds, and as such, insufficient influx will not benefit the patch. Obviously, such phenomenon cannot be revealed by the model in Heffernan et al. (2014). We believe that our findings in terms of patch-based models can offer public health policy makers some insights on the prevention and control of Lyme disease transmission.

Although this study is limited to the case of unidirectional migration route, based on some reasonable hypothesis, our model can be extended for the entire migration chain of migratory birds including spring migration, summer breeding, fall migration and winter feeding, provided that we assume that birds at patch N all go back to patch 1 (except for deaths during migration) by replacing $\alpha^l_{0,1}(t)m_{0,1}(t-\tau_0)x_{0,5b}(t-\tau_0)$ and $\alpha^n_{0,1}(t)m_{0,1}(t-\tau_0)x_{0,8b}(t-\tau_0)$ with $\alpha^l_{N,1}(t)m_{N,1}(t-\tau_N)x_{N,5b}(t-\tau_N)$ and $\alpha^n_{N,1}(t)m_{N,1}(t-\tau_N)x_{N,8b}(t-\tau_N)$, and $m_{N,N+1}(t)$ with $m_{N,1}(t)$. In a future work,

as real bird migration data become available, utilizing the corresponding model of the full bird migration, we would like to estimate the real range expansion of the tick population in Canada, which remains a big challenge.

Acknowledgments This research was supported by NSERC of Canada and by the European Union and the State of Hungary, co-financed by the European Social Fund in the framework of the TÁMOP 4.2.4. A/2-11-1-2012-0001 "National Excellence Programme." GR was also supported by ERC Starting Grant No. 259559 and OTKA K109782. We thank Dr. Patrick A. Leighton at Université de Montréal for valuable discussion of parameter estimation and Dr. Nicholas Ogden at Public Health Agency of Canada for sharing the tick data. We would also like to thank the three anonymous referees for their helpful/useful comments which have helped us improve the presentation in the revision.

Appendix 1: Derivation of Model (1)

In the model (1), the key terms are those accounting for the influxes of feeding ticks (larvae and nymphs) between patches, because the other terms are almost self-explanatory and easy to understand. These terms are results of bird migration and thus need to be carefully derived by the tracking the bird migration and feeding age of ticks on flying birds. We illustrate the procedure by considering the feeding nymphs; the influx of feeding larvae can be obtained in a similar way.

The change rates of feeding nymphs infesting on birds in a particular patch consist of five components: development from local patch coming from the questing stage, immigration from the previous patch carried by migratory birds, emigration out of the patch to the next by the aid of migratory birds, development into the next stage and mortality. In order to formulate the equation of feeding nymphs on birds, we let $B_i(t)$ be the population of migratory birds at time t in patch i and $m_{i,i+1}(t)$ be migration rate of birds leaving patch i and flying to patch $i+1$. Let $u_i(t,a)$ be density of feeding nymphs infesting on birds at time t with feeding age a in patch i. By the meaning of $u_i(t,a)$, it is obvious that at a given time t within patch i, the total number of feeding nymphs on birds is given by

$$x_{i,8b}(t) = \int_0^\infty u_i(t,a)\,\mathrm{d}a. \tag{22}$$

For $0 \le a < \tau_{i-1}$, there is no feeding nymphs entering patch i from the previous patch due to the time delay in flight. Following the first principle governing the growth of a population with age structure, the density $u_i(t,a)$ ($i \in \mathcal{A}$) satisfies

$$\begin{cases} \left(\frac{\partial}{\partial t} + \frac{\partial}{\partial a}\right) u_i(t,a) &= -d_{i,8b}(t)u_i(t,a) \\ & \quad -m_{i,i+1}(t)u_i(t,a) - \mu_{i,8b}(t, x_{i,8b}(t))u_i(t,a), \\ u_i(t,0) &= d_{i,7b}(t, B_i(t))x_{i,7}(t). \end{cases} \tag{23}$$

For $\tau_{i-1} \le a < \infty$, migratory birds are capable of dispersing *I. scapularis* into patch i from the previous patch $i-1$. Then $u_i(t,a)$ at the given time t in patch i ($i \in \mathcal{A}$)

satisfies

$$\begin{aligned}&\left(\frac{\partial}{\partial t}+\frac{\partial}{\partial a}\right)u_i(t,a)\\&=-d_{i,8b}(t)u_i(t,a)-m_{i,i+1}(t)u_i(t,a)-\mu_{i,8b}(t,x_{i,8b}(t))u_i(t,a)\\&\quad+[\text{influx of feeding nymphs at time } t \text{ with age } a].\end{aligned}\tag{24}$$

We need to derive the influx term on the right side in (24). The idea is to use the method of the characteristics, just as in Gourley et al. (2010). Let $l_{i-1,i}$ be the distance along the flyway from patch $i-1$ to patch i and $v_{i-1,i}$ be the average flying velocity of the birds flying from patch $i-1$ to patch i. Then the time for a *I. scapularis* to be carried from patch $i-1$ to patch i is $\tau_{i-1}=l_{i-1,i}/v_{i-1,i}$. Denote by $\mu^l_{i-1,i}(t)$, $\mu^n_{i-1,i}(t)$ and $\mu^b_{i-1,i}(t)$ the mortalities of per capita feeding larvae, feeding nymphs and migratory birds, respectively, and let $d^l_{i-1,i}(t)$ and $d^n_{i-1,i}(t)$ be the respective development rates of feeding larvae and feeding nymphs on birds.

Now, let

$$\begin{aligned}&\rho_{i-1,i}(t,a,y)\\&=\text{density of feeding nymphs on birds in the air along the route from patch } i-1\\&\quad\text{to patch } i \text{ at time } t \text{ with feeding age } a \text{ at location } y\in(0,l_{i-1,i}).\end{aligned}$$

Then $\rho_{i-1,i}(t,a,y)$ satisfies the reaction-advection equation

$$\begin{cases}\left(\frac{\partial}{\partial t}+\frac{\partial}{\partial a}\right)\rho_{i-1,i}(t,a,y) &= -v_{i-1,i}\frac{\partial\rho_{i-1,i}(t,a,y)}{\partial y}-\mu^b_{i-1,i}(t)\rho_{i-1,i}(t,a,y)\\ &\quad -\mu^n_{i-1,i}(t)\rho_{i-1,i}(t,a,y)-d^n_{i-1,i}(t)\rho_{i-1,i}(t,a,y),\\ v_{i-1,i}\rho_{i-1,i}(t,a,0) &= m_{i-1,i}(t)u_{i-1}(t,a).\end{cases}\tag{25}$$

with $m_{i-1,i}(t)u_{i-1}(t,a)$ being the flux of feeding nymphs leaving patch $i-1$ at time t. Then, the flux of feeding nymphs arriving at patch i at time t with age a is $v_{i-1,i}\rho_{i-1,i}(t,a,l_{i-1,i})$, which needs to be determined. For simplicity of notations, we denote $\gamma^n_{i-1,i}(t):=\mu^b_{i-1,i}(t)+\mu^n_{i-1,i}(t)+d^n_{i-1,i}(t)$ $(i=2,\ldots,N)$, which exactly indicates the removal rate of feeding nymphs in the air along the route from patch $i-1$ and patch i. Since time and age advance at the same rate, we let

$$S(t,y,r)=\rho_{i-1,i}(t,t+r,y)\tag{26}$$

for any given real number r. By differentiating $S(t,y,r)$ with respect to time t, we obtain

$$\begin{aligned}\frac{\partial S}{\partial t}(t,y,r)&=\left[\frac{\partial\rho_{i-1,i}}{\partial t}(t,a,y)+\frac{\partial\rho_{i-1,i}}{\partial a}(t,a,y)\right]_{a=t+r}\\&=-v_{i-1,i}\frac{\partial\rho_{i-1,i}}{\partial y}(t,t+r,y)-\gamma^n_{i-1,i}(t)\rho_{i-1,i}(t,t+r,y).\end{aligned}$$

So that

$$\frac{\partial S}{\partial t}(t,y,r) = -v_{i-1,i}\frac{\partial S}{\partial y}(t,y,r) - \gamma^n_{i-1,i}(t)S(t,y,r).$$

Denote $S_\xi(y,r) = S(\xi + \frac{y}{v_{i-1,i}}, y, r)$. Then $S_\xi(y,r)$ satisfies the following equation

$$\begin{aligned}\frac{\mathrm{d}S_\xi(y,r)}{\mathrm{d}y} &= \left(\frac{\partial S}{\partial t}\frac{\partial t}{\partial y} + \frac{\partial S}{\partial y}\right)\Big|_{t=\xi+\frac{y}{v_{i-1,i}}} \\ &= \frac{1}{v_{i-1,i}}\left(\frac{\partial S}{\partial t} + v_{i-1,i}\frac{\partial S}{\partial y}\right)\Big|_{t=\xi+\frac{y}{v_{i-1,i}}} \\ &= -\frac{1}{v_{i-1,i}}\gamma^n_{i-1,i}\left(\xi + \frac{y}{v_{i-1,i}}\right)S_\xi(y,r). \end{aligned} \tag{27}$$

The above Eq. (27) is a linear first-order ordinary differential equation. Integrating equation (27) with respect to the variable y from 0 to $l_{i-1,i}$ yields

$$S_\xi(l_{i-1,i},r) = S_\xi(0,r)\exp\left(\frac{-1}{v_{i-1,i}}\int_0^{l_{i-1,i}}\gamma^n_{i-1,i}(t)\,\mathrm{d}y\right).$$

Setting $\xi = t - \frac{l_{i-1,i}}{v_{i-1,i}}$ and letting $\eta = \xi + \frac{y}{v_{i-1,i}}$ along with the fact $\tau_{i-1} = \frac{l_{i-1,i}}{v_{i-1,i}}$, we obtain

$$\begin{aligned} S(t,l_{i-1,i},r) &= S(t-\tau_{i-1},0,r)\exp\left(-\frac{1}{v_{i-1,i}}\int_0^{l_{i-1,i}}\gamma^n_{i-1,i}\left(\xi+\frac{y}{v_{i-1,i}}\right)\mathrm{d}y\right) \\ &= S(t-\tau_{i-1},0,r)\exp\left(-\frac{1}{v_{i-1,i}}\int_0^{l_{i-1,i}}\gamma^n_{i-1,i}\left(t+\frac{y-y_i}{v_{i-1,i}}\right)\mathrm{d}y\right) \\ &= S(t-\tau_{i-1},0,r)\exp\left(-\int_{t-\tau_{i-1}}^{t}\gamma^n_{i-1,i}(\eta)\,\mathrm{d}\eta\right) \\ &:= S(t-\tau_{i-1},0,r)\alpha^n_{i-1,i}(t), \end{aligned}$$

where

$$\alpha^n_{i-1,i}(t) := \exp\left(-\int_{t-\tau_{i-1}}^{t}(\mu^n_{i-1,i}(\eta) + \mu^b_{i-1,i}(\eta) + d^n_{i-1,i}(\eta))\,\mathrm{d}\eta\right) \tag{28}$$

which accounts for the probability that a feeding nymph can survive the flight from patch $i-1$ to patch i. Thus,

$$\rho_{i-1,i}(t,a,y_i) = \rho_{i-1,i}(t-\tau_{i-1}, a-\tau_{i-1}, y_{i-1})\alpha^n_{i-1,i}(t). \tag{29}$$

Then, the flux of feeding nymphs at time t with age a entering patch i is given by

$$\begin{aligned} &v_{i-1,i}\rho_{i-1,i}(t,a,y_i) = v_{i-1,i}\rho_{i-1,i}(t-\tau_{i-1}, a-\tau_{i-1}, y_{i-1})\alpha^n_{i-1,i}(t) \\ &\quad = [\text{outward flux in patch } i-1 \text{ at time } t-\tau_{i-1} \text{ of age } a-\tau_{i-1}] \times \alpha^n_{i-1,i}(t) \\ &\quad = \alpha^n_{i-1,i}(t)m_{i-1,i}(t-\tau_{i-1})u_{i-1}(t-\tau_{i-1}, a-\tau_{i-1}). \end{aligned}$$

Summarizing the above, $u_i(t,a)$ satisfies

$$\left(\frac{\partial}{\partial t}+\frac{\partial}{\partial a}\right)u_i(t,a) = \begin{cases} -d_{i,8b}(t)u_i(t,a) - m_{i,i+1}(t)u_i(t,a) \\ -\mu_{i,8b}(t,x_{i,8b}(t))u_i(t,a), \quad 0 \le a < \tau_{i-1} \\ \\ \alpha^n_{i-1,i}(t)m_{i-1,i}(t-\tau_{i-1})u_{i-1}(t-\tau_{i-1},a-\tau_{i-1}) \\ -d_{i,8b}(t)u_i(t,a) \qquad\qquad \tau_{i-1} \le a < \infty, \\ -m_{i,i+1}(t)u_i(t,a) - \mu_{i,8b}(t,x_{i,8b}(t))u_i(t,a), \end{cases} \tag{30}$$

with $\alpha^n_{i-1,i}(t)$ given by (28).

Taking derivative in Eq. (22) and making use of (30) yield

$$\begin{aligned} x'_{i,8b}(t) &= \int_0^{\tau_{i-1}} \frac{\partial}{\partial t}u_i(t,a)\,\mathrm{d}a + \int_{\tau_{i-1}}^{\infty}\frac{\partial}{\partial t}u_i(t,a)\,\mathrm{d}a \\ &= \int_0^{\tau_{i-1}}\left(\frac{\partial}{\partial t}+\frac{\partial}{\partial a}\right)u_i(t,a)\,\mathrm{d}a + u_i(t,0) - u_i(t,\tau_{i-1}) \\ &\quad + \int_{\tau_{i-1}}^{\infty}\left(\frac{\partial}{\partial t}+\frac{\partial}{\partial a}\right)u_i(t,a)\,\mathrm{d}a + u_i(t,\tau_{i-1}) - u_i(t,\infty) \\ &= u_i(t,0) + \alpha^n_{i-1,i}(t)m_{i-1,i}(t-\tau_{i-1})x_{i-1,8b}(t-\tau_{i-1}) \\ &\quad - d_{i,8b}(t)x_{i,8b}(t) - m_{i,i+1}(t)x_{i,8b}(t) - \mu_{i,8b}(t,x_{i,8b}(t))x_{i,8b}(t) \\ &= \underbrace{d_{i,7b}(t,B_i(t))x_{i,7}(t)}_{\text{attachment from local patch}} + \underbrace{\alpha^n_{i-1,i}(t)m_{i-1,i}(t-\tau_{i-1})x_{i-1,8b}(t-\tau_{i-1})}_{\text{immigration from previous patch}} \\ &\quad - \underbrace{d_{i,8b}(t)x_{i,8b}(t)}_{\text{development to the next}} - \underbrace{m_{i,i+1}(t)x_{i,8b}(t)}_{\text{emigration out of the patch}} - \underbrace{\mu_{i,8b}(t,x_{i,8b}(t))x_{i,8b}(t)}_{\text{density-dependent death}}, \end{aligned} \tag{31, 32}$$

where we have made the biologically realistic assumption $u_i(t,\infty)=0$.

In a similar way, we obtain the dynamics of feeding larvae on birds at patch i as below

$$\begin{aligned} x'_{i,5b}(t) &= \underbrace{d_{i,4b}(t,B_i(t))x_{i,4}(t)}_{\text{attachment from local patch}} + \underbrace{\alpha^l_{i-1,i}(t)m_{i-1,i}(t-\tau_{i-1})x_{i-1,5b}(t-\tau_{i-1})}_{\text{immigration from previous patch}} \\ &\quad - \underbrace{d_{i,5b}(t)x_{i,5b}(t)}_{\text{development to the next}} - \underbrace{m_{i,i+1}(t)x_{i,5b}(t)}_{\text{emigration out of the patch}} - \underbrace{\mu_{i,5b}(t,x_{i,5b}(t))x_{i,5b}(t)}_{\text{density-dependent death}}, \end{aligned} \tag{33}$$

where

$$\alpha^l_{i-1,i}(t) = \exp\left(-\int_{t-\tau_{i-1}}^{t}\left(\mu^b_{i-1,i}(\eta)+\mu^l_{i-1,i}(\eta)+d^l_{i-1,i}(\eta)\,\mathrm{d}\eta\right)\right)$$
$$:= \exp\left(-\int_{t-\tau_{i-1}}^{t}\gamma^l_{i-1,i}(\eta)\,\mathrm{d}\eta\right). \tag{34}$$

Therefore, for $t > \max\{\tau_1, \tau_2, \ldots, \tau_{N-1}\}$, we have derived the closed system (1) for tick dynamics over N patches with migration birds. For $t \in [0, \tau_{i-1}]$, the dynamics of *I. scapularis* tick population is governed by an ODE system obtained by simply deleting the two delayed terms in (1). Since we are concerned with the long-term dynamics of ticks, we only need to analyze the model system (1), as is done in the main text.

Appendix 2: Proof of Lemma 6.1

Let $A(t) = F(t) - V(t)$. It is obvious that all off-diagonal entries are nonnegative and hence the linear system (11) is cooperative. But it may not be irreducible since some parameters may vanish in some nonempty subinterval due to seasonal activities of ticks and birds. This means that the semiflow $\Phi_A(t)$ generated by system (11) may not be strongly monotone for all $t > 0$. However, next lemma shows that $\Phi_A(t)$ is *eventually strongly monotone*.

Lemma 6.1 *The solution semiflow $X(t) = \Phi_A(t)$ of (11) is nonnegative for all $t \geq 0$ and is positive for $t \geq 12\omega$.*

Proof Since (11) is a cooperative system, Corollary B.2 on page 262 of Smith and Waltman (1995) implies that $X(t) = [x_{i,j}(t)]_{14\times 14} \geq 0$ for all $t \geq 0$.

Note that $X(t)$ is the fundamental matrix solution of (11) satisfying

$$\begin{cases} X'(t) = A(t)X(t) = (a_{i,j}(t))_{14\times 14}X(t) \\ X(0) = I \quad \text{(the identity matrix)} \end{cases} \tag{35}$$

Since all off-diagonal entries of $A(t)$ are nonnegative, a comparison theorem implies that once an entry of $X(t)$ becomes strictly positive at some time, it will remain strictly positive after that time. Next, we show that each component of $X(t)$ will actually be turned on at some $t \geq 0$. We start by considering x_{21}. According to the first equation of (35), we have

$$x'_{2,1}(t) = \sum_{k=1}^{14} a_{2,k}(t)x_{k,1}(t) = p(t)f(0)x_{1,1}(t) - \mu_{2,1}(t)x_{2,1}(t) \tag{36}$$

and $x_{1,1}(0) = 1 > 0$. Since $x_{2,1}(0) = 0$ and $x'_{2,1}(0) = p(t)f(0)x_{1,1}(0) = p(t)f(0) > 0$, we know that there is a $t^* \in [0, \omega]$ such that $x_{1,1}(t) = 1 > 0$ for

$t \in (0, t^*]$, and by the above argument, we conclude that $x_{1,1}(t) = 1 > 0$ for all $t \geq t^*$, particularly for $t \geq w$. Next, we look at $x_{3,1}(t)$ which satisfies

$$x'_{3,1}(t) = \sum_{k=1}^{14} a_{3,k}(t)x_{k,1}(t) = d_{1,2}(t)x_{2,1}(t) - (d_{1,3}(t) + \mu_{1,3}(t))x_{3,1}(t). \quad (37)$$

By the positivity of $x_{2,1}(t)$ for $t \geq w$ and using the constant-variation formula, we know that $x_{3,1}(t)$ becomes positive at some time for $[\omega, 2\omega]$ and hence $x_{2,1}(t)$ is strictly positive for $t \geq 2\omega$. Going over the rest of the components in a similar way, we can conclude that $x_{i,j} > 0$ for $t \geq k\omega$ where $k\omega$ is the number in the (i, j) position of the following matrix:

$$\begin{pmatrix}
0 & 11\omega & 10\omega & 9\omega & 8\omega & 8\omega & 7\omega & 6\omega & 5\omega & 5\omega & 4\omega & 3\omega & 2\omega & \omega \\
\omega & 0 & 11\omega & 10\omega & 9\omega & 9\omega & 8\omega & 7\omega & 6\omega & 6\omega & 5\omega & 4\omega & 3\omega & 2\omega \\
2\omega & \omega & 0 & 11\omega & 10\omega & 10\omega & 9\omega & 8\omega & 7\omega & 7\omega & 6\omega & 5\omega & 4\omega & 3\omega \\
3\omega & 2\omega & \omega & 0 & 11\omega & 11\omega & 10\omega & 9\omega & 8\omega & 8\omega & 7\omega & 6\omega & 5\omega & 4\omega \\
4\omega & 3\omega & 2\omega & \omega & 0 & 12\omega & 11\omega & 10\omega & 9\omega & 9\omega & 8\omega & 7\omega & 6\omega & 5\omega \\
4\omega & 3\omega & 2\omega & \omega & 12\omega & 0 & 11\omega & 10\omega & 9\omega & 9\omega & 8\omega & 7\omega & 6\omega & 5\omega \\
5\omega & 4\omega & 3\omega & 2\omega & \omega & \omega & 0 & 11\omega & 10\omega & 10\omega & 9\omega & 8\omega & 7\omega & 6\omega \\
6\omega & 5\omega & 4\omega & 3\omega & 2\omega & 2\omega & \omega & 0 & 11\omega & 11\omega & 10\omega & 9\omega & 8\omega & 7\omega \\
7\omega & 6\omega & 5\omega & 4\omega & 3\omega & 3\omega & 2\omega & \omega & 0 & 12\omega & 11\omega & 10\omega & 9\omega & 8\omega \\
7\omega & 6\omega & 5\omega & 4\omega & 3\omega & 3\omega & 2\omega & \omega & 12\omega & 0 & 11\omega & 10\omega & 9\omega & 8\omega \\
8\omega & 7\omega & 6\omega & 5\omega & 4\omega & 4\omega & 3\omega & 2\omega & 1\omega & 1\omega & 0 & 11\omega & 10\omega & 9\omega \\
9\omega & 8\omega & 7\omega & 6\omega & 5\omega & 5\omega & 4\omega & 3\omega & 2\omega & 2\omega & \omega & 0 & 11\omega & 10\omega \\
10\omega & 9\omega & 8\omega & 7\omega & 6\omega & 6\omega & 5\omega & 4\omega & 3\omega & 3\omega & 2\omega & \omega & 0 & 11\omega \\
11\omega & 10\omega & 9\omega & 8\omega & 7\omega & 7\omega & 6\omega & 5\omega & 4\omega & 4\omega & 3\omega & 2\omega & \omega & 0
\end{pmatrix}.$$

The proof is completed. □

References

Anderson JF (1988) Mammalian and avian reservoirs for Borrelia burgdorferi. Ann N Y Acad Sci 539:180–191

Bacaër N (2007) Approximation of the basic reproduction number $\mathcal{R}_0$ for vector-borne diseases with a periodic vector population. Bull Math Biol 69:1067–1091

Bacaër N, Guernaoui S (2006) The epidemic threshold of vector-borne diseases with seasonality: the case of cutaneous leishmaniasis in Chichaoua, Morocco. J Math Biol 53:421–436

Bird Life International (2013) Species factsheet: Turdus migratorius. http://www.birdlife.orgon20/02/2013

Bourouiba L, Wu J, Newman S, Takekawa J, Natdorj T, Batbayar N, Bishop CM, Hawkes LA, Butler PJ, Wikelski M (2010) Spatial dynamics of bar-headed geese migration in the context of H5N1. J R Soc Interface 7:1627–1639

Brinkerhoff RJ, Folsom-O'keefe CM, Tsao K, Diuk-Wasser MA (2011) Do birds affect Lyme disease risk? Range expansion of the vector-borne pathogen Borrelia burgdorferi. Front Ecol Environ 9:103–110

Centers for Disease Control and Prevention (2014) Reported cases of Lyme disease by state or locality (CDC2014) 2003–2012

Comstedt P, Bergstrom S, Olsen B, Garpmo U, Marjavaara L, Mejlon H, Barbour AG, Bunikis J (2006) Migratory passerine birds as reservoirs of Lyme borreliosis in Europe. Emerg Infect Dis 12:1087–1095

Gourley SA, Liu R, Wu J (2010) Spatiotemperature distributions of Migratory birds: patchy model with delay. SIAM J Appl. Dyn. Syst. 9(2):589–610

Hale JK, Verduyn Lunel SM (1993) Introduction to functional differential equations. Springer, New York

Hasle G, Bjune GA, Midthjell L, Røed KH, Leinaas HP (2011) Transport of *Ixodes ricinus* infected with Borrelia species to Norway by northward-migrating passerine birds. Ticks Tick Borne Dis 2:37–43

Heffernan JM, Lou Y, Wu J (2014) Range expansion of *Ixodes scapularis* ticks and of *Borrelia burgdorferi* by migratory birds. Discrete Contin Dyn Syst Ser B 19:3147–3167

Madhav NK, Brownstein JS, Tsao JI, Fish D (2004) A dispersal model for the range expansion of blacklegged tick (Acari: Ixodidae). J Med Entomol 41(5):842–852

Morshed MG, Scott JD, Fernando K, Beati L, Mazerolle DF, Geddes G, Durden LA (2005) Migratory songbirds disperse ticks across Canada, and first isolation of the Lyme disease spirochete, Borrelia burgdorferi, from the avian tick, Ixodes auritulus. J Parasitol 91:780–790

Nakata Y, Röst G (2015) Global analysis for spread of infectious diseases via transportation networks. J Math Biol 70:1411–1456

Ogden NH, Lindsay LR, Beauchamp G, Charron D, Maarouf A, O'Callaghan CJ, Waltner-Toews D, Barker TK (2004) Investigation of relationships between temperature and developmental rates of tick *Ixodes scapularis* (Acari: Ixodidae) in the laboratory and field. J Med Entomol 41:622–633

Ogden NH, Bigras-Poulin M, O'Callaghan C, Barker I, Lindsay L, Maarouf A, Smoyer-Tomic K, Waltner-Toews D, Charron D (2005) A dynamic population model to investigate effects of climate on geographic range and seasonality of the tick *Ixodes scapularis*. Int J Parasitol 35:375–389

Ogden NH, Maarouf A, Barker IK, Bigras-Poulin M, Lindsay LR, Morshed MG, O'callaghan CJ, Ramay F, Waltner-Toews D, Charron DF (2006) Climate change and the potential for range expansion of the Lyme disease vector *Ixodes scapularis* in Canada. Int J Parasitol 36:63–70

Ogden NH, Lindsay LR, Hanincoá K, Barker IK, Bigras-Poulin M, Charron DF, Heagy A, Francis CM, O'Callaghan CJ, Schwartz I, Thompson RA (2008) Role of migratory birds in introduction and range expansion of *Ixodes scapularis* ticks and of *Borrelia burgdorferi* and *Anaplasma phagocytophilum* in Canada. Appl Environ Microbiol 74:1780–1790

Ogden NH, Lindsay LR, Morshed M, Sockett PN, Artsob H (2008) The rising challenge of Lyme borreliosis in Canada. Can Commun Dis Rep 34(1):1–19

Ogden NH, St-Onge L, Barker IK, Brazeau S, Bigras-Poulin M, Charron DF, Francis CM, Heagy A, Lindsay LR, Maarouf A, Michel P, Milord F, O'callaghan CJ, Trudel L, Thompson RA (2008) Risk maps for range expansion of the Lyme disease vector, *Ixodes scapularis*, in Canada now and with climate change. Int J Health Geogr 7:24

Ogden NH, Lindsay LR, Morshed M, Sockett PN, Artsob H (2009) The emergence of Lyme disease in Canada. CMAJ 180:1221–1224

Ogden NH, Radojevic M, Wu X, Duvvuri VR, Leighton PA, Wu J (2014) Estimated effects of projected climate change on the basic reproductive number of the Lyme disease vector *Ixodes scapularis*. Environ Health Perspect 122:631–638

Rand PW, Lacombe EH Jr, Smith RP, Ficker J (1998) Participation of birds (Aves) in the emergence of Lyme disease in Southern Maine. J Med Entomol 35:270–276

Robin Migration Study (2015) Annenberg Learner. http://www.learner.org/jnorth/tm/robin/FAQSAutumn.html. Accessed 10 Sep 2015

Smith HL (1995) Monotone dynamical systems: an introduction to the theory of competitive and cooperative systems. Mathematical Surveys and Monographs 41. AMS, Providence, RL

Smith HL, Waltman P (1995) The theory of the chemostat: dynamics of microbial competition. Cambridge University Press, Cambridge

Wang W, Zhao X-Q (2008) Threshold dynamics for compartmental epidemic models in periodic environments. J Dyn Differ Equ 20:699–717

Wu X, Wu J (2012) Diffusive systems with seasonality: eventually strongly order-preserving periodic processes and range expansion of tick populations. Can Appl Math Q 20:557–586

Wu X, Duvvri VR, Lou Y, Ogden NH, Pelcat Y, Wu J (2013) Developing a temperature-driven map of the basic reproductive number of the emerging tick vector of Lyme disease *Ixodes scapularis* in Canada. J Theor Biol 319:50–61

Zhang F, Zhao X-Q (2008) A periodic epidemic model in a patchy environment. J Math Anal Appl 325:496–516

Zhao X-Q (2003) Dynamical systems in population biology. Springer, New York

Zhao X-Q, Jing Z (1996) Global asymptotic behavior in some cooperative systems of functional-differential equations. Can Appl Math Q 4:421–444